

Revised stratigraphy of the Stuhini and Hazelton groups and LA-ICP-MS zircon geochronology of the Scottie gold mine area, northwestern British Columbia



Ben Stanley^{1, a} and JoAnne Nelson²

¹Scottie Resources Corp., 905-1111 West Hastings Street, Vancouver, BC, V6E 2J3

²Emeritus Scientist, British Columbia Geological Survey, Ministry of Energy, Mines and Low Carbon Innovation, Victoria, BC, V8W 9N3

^acorresponding author: Stanley@seracx.com

Recommended citation: Stanley, B., and Nelson, J., 2022. Revised stratigraphy of the Stuhini and Hazelton groups and LA-ICP-MS zircon geochronology of the Scottie gold mine area, northwestern British Columbia. In: Geological Fieldwork 2021, British Columbia Ministry of Energy, Mines and Low Carbon Innovation, British Columbia Geological Survey Paper 2022-01, pp. 83-102.

Abstract

The past-producing Scottie gold mine lies within the Stewart mining camp, in the southern part of a prolific mineral district in northwestern British Columbia popularly known as the 'Golden Triangle'. The Golden Triangle includes Cu-Au porphyries (e.g., Red Chris, KSM), epithermal gold deposits (e.g., Brucejack, Scottie Gold) and VMS deposits (e.g., Eskay Creek, Granduc, Anyox). They are hosted by, and causally related to, Upper Triassic through Middle Jurassic volcano-sedimentary strata of the Stuhini and Hazelton groups and/or comagmatic subvolcanic intrusions, and many are spatially related to the unconformable contact between the Stuhini Group and overlying Hazelton Group. In this study, detailed geological mapping, supported by geochemistry and LA-ICP-MS zircon geochronology of volcanic and sedimentary units, establish a stratigraphic section through the upper Stuhini and lower Hazelton groups in the Scottie gold mine area.

Recognized for the first time in this study, the Stuhini Group in the Stewart mining camp includes a lower unit of interlayered argillite, limestone, plagioclase-rich fine-grained sandstone and felsic tuff, which grades up-section into an upper volcanic unit of augite-phyric trachyandesite (latite) breccias, flows and flow-breccias, and felsic (trachyte) flows, lapilli- and crystal lithic tuffs. Geochemically the volcanic rocks are highly potassic, of shoshonitic affinity. Zircons from a crystal tuff near the base of the upper volcanic unit yielded a Youngest Statistical Population (YSP) weighted average of 214.2 ± 1.0 Ma, considered the age of crystallization.

Hazelton Group stratigraphy in the Stewart mining camp is comparable to but distinct from that in the McTagg anticlinorium. The stratigraphically lowest unit in the Hazelton Group forms an isolated exposure of beige siltstone with lesser interbeds of sandstone and mudstone, apparently overlying sedimentary strata of the lower Stuhini Group unit across an ice-covered contact. Zircons from a siltstone in this unit yielded a YSP weighted average age of 201.0 ± 5.2 Ma, which we interpret as the maximum age for the onset of Hazelton Group deposition in this area. It coincides with a ca. 200.5 Ma U-Pb zircon age of the nearby Tennyson porphyry, interpreted as comagmatic with early Hazelton volcanism, and with the Hettangian-Sinemurian faunal age of the Jack Formation at the base of the Hazelton Group on the flanks of the McTagg anticlinorium, 20 kilometres to the north. In the eastern half of the map area, steeply dipping strata of the Betty Creek Formation (lower Hazelton Group) paraconformably overlie the upper Stuhini volcanic unit. The Betty Creek Formation includes two intervals of feldspar-hornblende-phyric andesitic flows, tuffs, breccias, and conglomerates of the Unuk River andesite unit, separated by a siltstone unit that contains a Pliensbachian(?) ammonite mold and has yielded a YSP weighted average of 190.6 ± 1.7 Ma. These ages correspond to the latter stages of Betty Creek volcanism on the flanks of the McTagg anticlinorium.

The highly diverse metallogeny of the Golden Triangle resulted from collision-driven processes during Stuhini and Hazelton arc and back-arc development. The New Britain arc and Bismarck plate provide a modern analogue of collision-related arc and back-arc reorganization, which has given rise to both alkalic Cu-Au porphyries (Lihir) and seabed massive sulphide deposits (Manus basin). The upper volcanic unit in the Stuhini Group, described here, provides new evidence of shoshonitic volcanism at the transition from main-stage Stuhini arc-back-arc activity into post-collision (Galore suite) magmatism.

Keywords: Scottie gold mine, Stewart mining camp, Stuhini Group, Hazelton Group, detrital zircon geochronology, litho-geochemistry, shoshonite

1. Introduction

The Golden Triangle is the popular name for a large, prolific mineral district in northwestern British Columbia, in which Cu-Au and Cu-Mo porphyries, precious metal vein systems, and volcanogenic massive sulphide deposits are hosted by Late Triassic to Middle Jurassic volcano-sedimentary successions and cogenetic intrusions (Fig. 1 inset; Nelson and van Straaten, 2021). The stratigraphic setting of these deposits is a key

aspect of their metallogeny, with many of them within 2 km of the unconformable contact between the Stuhini Group and overlying uppermost Triassic to Jurassic rocks of the Hazelton Group. In the last decades, discovery and development of the Brucejack gold mine and the KSM (Kerr-Sulphurets-Mitchell) Cu-Au porphyry resource in the McTagg anticlinorium (Fig. 1) has been accompanied by intensive geological study by government and university researchers. Detailed geological

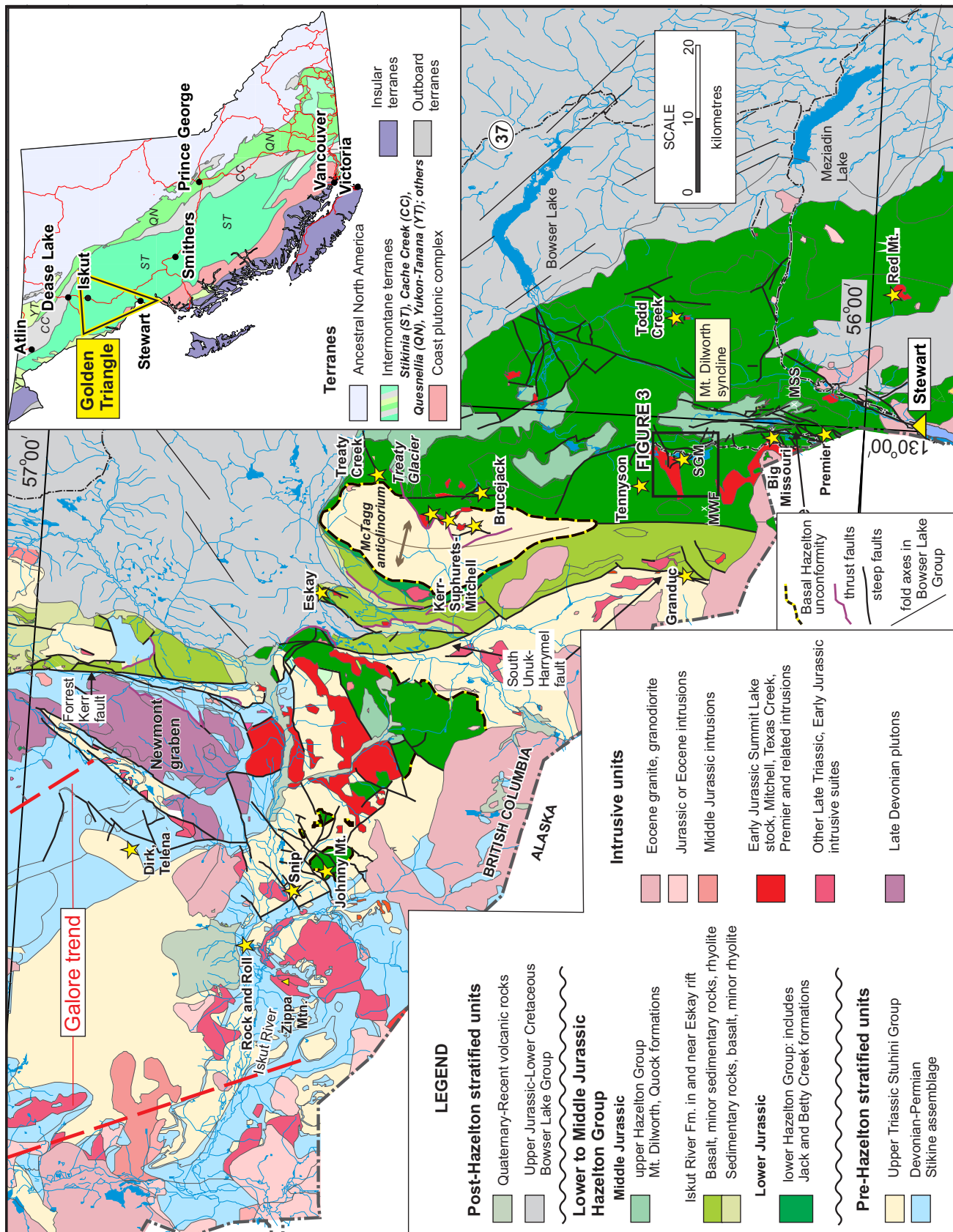


Fig. 1. Regional setting of the Scottie gold mine area in the southern Iskut River region of northwestern British Columbia. Inset, generalized terrane map and position at southern tip of the Golden Triangle. SGM = Scottie Gold Mine; MWF = Mt. White-Fraser; MSS = Mt. Shorty-Stevenson.

mapping, stratigraphic, and geochronological studies have shown important temporal and spatial relationships between Cu-porphyry and precious metal vein mineralization, Triassic-Jurassic intrusions, the sub-Hazelton Group unconformity surface, and favourable stratigraphic settings in the Hazelton Group (Lewis, 2013; Nelson and Kyba, 2014; Febbo et al., 2015; Tombe et al., 2018; Nelson et al., 2018; Fig. 1). In turn, these regional studies have led to terrane-scale tectonic and metallogenetic syntheses that depict evolving arc-back-arc configurations during terrane accretion to the North American margin (Nelson and van Straaten, 2021; Nelson et al., 2022, in press).

Before the present study, comparable stratigraphic and geochronological constraints have not been available for the Stewart mining camp, south of the McTagg anticlinorium (Fig. 1). The area has not been systematically mapped or studied since the 1980s. This contribution, based on detailed geological mapping of the Scottie gold mine area, documents for the first time a stratigraphic section of the upper Stuhini and lower Hazelton groups in the Stewart mining camp, with temporal constraints provided by LA-ICP-MS geochronology. It describes a previously unrecognized volcanic unit of shoshonite affinity in the upper part of the Stuhini Group, locates what may be the basal Hazelton unconformity, and aligns Hazelton Group stratigraphic subdivisions in this area with those established in the McTagg anticlinorium by Lewis (2013) and Nelson et al. (2018). These new observations clarify the tectonic history of the Stewart mining camp during the crucial transition between Stuhini and Hazelton arc and back-arc configurations. The Scottie property is within the traditional lands of the Nisga'a First Nation.

2. Regional geology

The study area lies within Stikinia, a multiphase arc-back-arc terrane constructed between the Late Devonian and Early Jurassic (Fig. 1; e.g., Nelson and van Straaten, 2021). Three unconformity-bounded island arc volcano-sedimentary successions are recognized: 1) the Stikine assemblage (upper Paleozoic; Logan et al., 2000; Gunning et al., 2006); 2) the Stuhini and Takla groups (Middle to Upper Triassic); and 3) the Hazelton Group (uppermost Triassic to Middle Jurassic; Nelson et al., 2018). Coeval and comagmatic Mesozoic arc-related intrusive suites include Late Triassic Stuhini Group equivalents (Stikine and Galore suites) and latest Triassic (Tatogga suite) and Early Jurassic (Texas Creek suite) Hazelton Group equivalents (Alldrick, 1993; Nelson et al., 2018; Nelson and van Straaten, 2021).

The main axis of Stuhini Group magmatism is defined by thick accumulations of mafic to intermediate volcanic rocks along the Stikine arch region of northern Stikinia (Brown et al., 1996; van Straaten and Wearmouth, 2019) and accompanying ca. 229-216 Ma Stikine suite plutons that form an easterly trend along the arch (Nelson and van Straaten, 2021). In contrast, Stuhini Group sections farther south, in the McTagg

anticlinorium and Stewart mining camp (Fig. 1), comprise mainly sedimentary units and augite-phyric to aphanitic basalts (Massey et al., 2005; Lewis, 2013), which Nelson and van Straaten (2021) infer were deposited in a marine back-arc basin.

The Stuhini Group near the Granduc volcanogenic massive sulphide deposit in the western part of the Stewart mining camp (Fig. 1) comprises phyllite and meta-clastic strata with thinner mafic interlayers that may be extrusive, intrusive or both (Lewis, 2013). A sheared mafic unit in the footwall of the Granduc deposit yielded a U-Pb zircon age of 222 ± 1 Ma, based on three concordant fractions (Childe, 1997). Detrital zircons from a heterolithic breccia in the hanging wall of the deposit gave an interpreted MDA (Maximum Depositional Age) of ca. 208 Ma (Mihalynuk et al., 2019), reinterpreted as $213.3 \pm 6.0/-4.8$ Ma, with exclusion of a single ca. 194 Ma youngest grain (Nelson and van Straaten, 2021). Based on the existing age constraints on Granduc (between 222 and 208 Ma) the volcanogenic mineralization either formed in a back-arc setting during main Stuhini arc-building at 229-216 Ma (Nelson and van Straaten, 2021), or after subduction ceased. The younger age is more likely, because the hanging wall breccia unit contains mineralized clasts that were interpreted as intraclasts (Mihalynuk et al., 2019).

A distinctive north-trending magmatic belt, the Galore trend, developed in western Stikinia between 212 and 203 Ma (Fig. 1; Nelson and van Straaten, 2021; Nelson et al., 2022 in press). The Galore plutonic suite that defines this trend is typified by small plutons and stocks of predominantly alkaline affinity. Comagmatic volcanic units include shoshonitic basalts and alkali-enriched pyroclastic deposits (Logan and Koyanagi, 1994). The southernmost known exposures of the Galore belt, in the lower Iskut River region, are: 1) the Zippa Mountain gabbro-syenite pluton (Fig. 1; Coulson et al., 1999, 2007); 2) small, ca. 214-203 Ma, mildly alkalic porphyritic stocks and diatremes and biotite-K-feldspar-bearing tuff and volcanic breccias interpreted as their extrusive equivalents, near the Dirk and Telena mineral occurrences (Fig. 1; Mihalynuk et al., 2011, 2012; Nelson and van Straaten, 2021) and 3) small Late Triassic syenite plutons in the Newmont graben (Fig. 1; Logan et al., 2000).

Stuhini arc and post-arc magmatic activity ceased by the latest Triassic due to collision of northern Stikinia and the pericratonic Yukon-Tanana terrane, which led to uplift and variable deformation throughout the terrane (Nelson and van Straaten, 2021; Nelson et al., 2022, in press). The base of the lower Hazelton Group is a regional unconformity that was initially recognized in the 1990s (e.g., Henderson et al., 1992; Brown et al., 1996; Logan et al., 2000) and has since become increasingly well documented (Greig, 2014; Nelson and Kyba, 2014; Kyba and Nelson, 2015; Febbo et al., 2019; Miller et al., 2020). The lower Hazelton Group (Rhaetian-Pliensbachian) represents the development of the Hazelton arc and its back-arc (Nelson et al., 2018). It is overlain by post-arc sedimentary and volcanic strata of the upper Hazelton Group (Pliensbachian-Callovia) including units of regional extent on the periphery

of the Bowser Basin and the volcano-sedimentary fill of the Eskay rift (Gagnon et al., 2012).

On the flanks of the McTagg anticlinorium (Fig. 1), the Stuhini Group-Hazelton Group contact is an angular unconformity (Nelson and Kyba, 2014), with the lowest unit in the Hazelton Group, the Jack Formation (Hettangian-Sinemurian), lying on previously tilted and, in some localities, folded Stuhini Group rocks (Fig. 2; Henderson et al., 1992; Lewis, 2013). The Jack Formation is overlain by the main volcanic unit of the lower Hazelton Group, the Betty Creek Formation (Lewis, 2013). The base of the Betty Creek Formation above

is compositionally mature relative to the Stuhini Group and apparently restricted to the McTagg area. It consists of cobble, highly rounded granitoid-clast conglomerate, quartz-bearing arkosic sandstone, granulestone, thinly bedded siltstones and mudstones and, west of the McTagg anticlinorium, a middle volcanoclastic unit (Nelson and Kyba, 2014).

The Jack Formation is overlain by the main volcanic unit of the lower Hazelton Group, the Betty Creek Formation (Lewis, 2013). The base of the Betty Creek Formation above

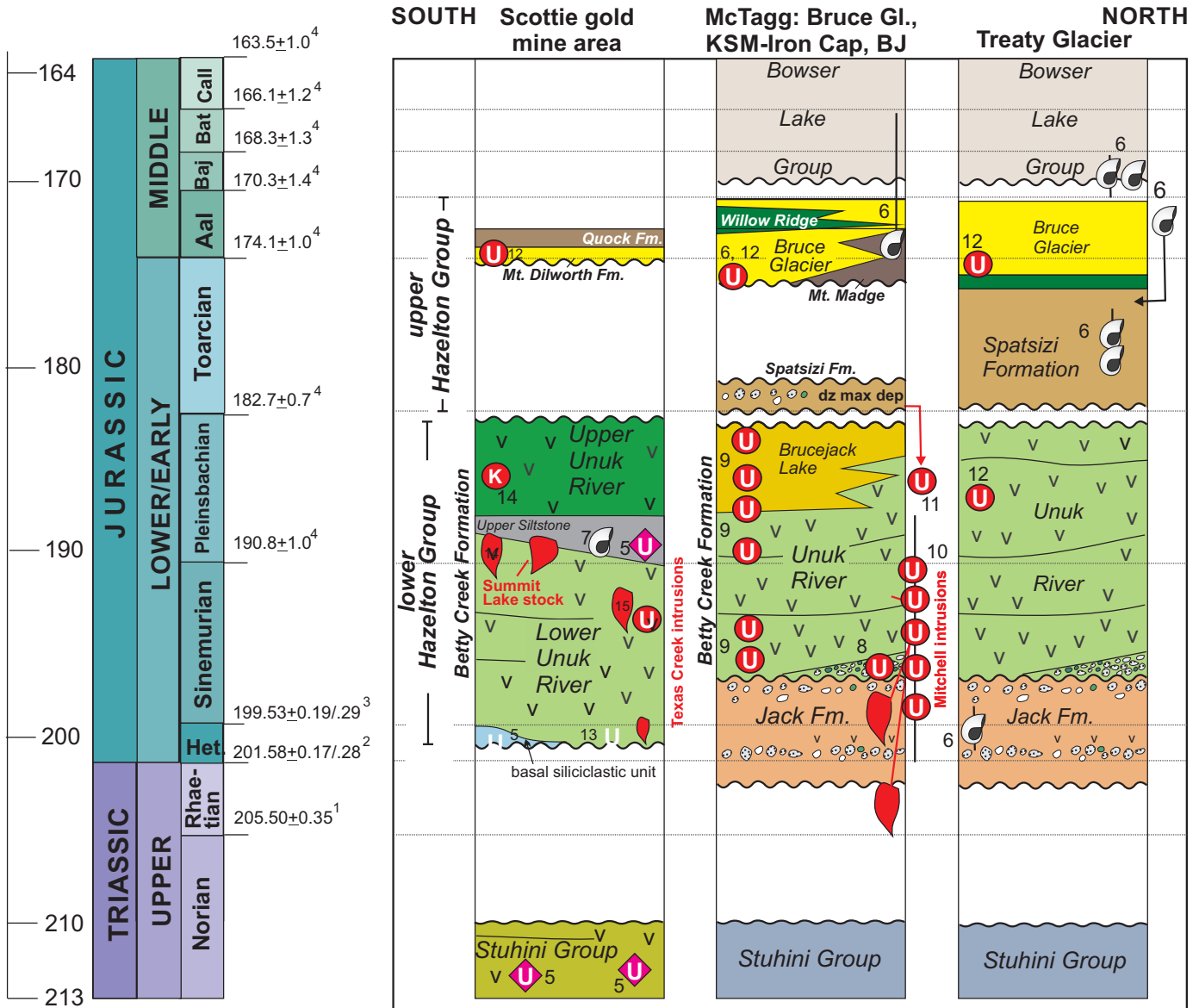


Fig. 2. Stratigraphic columns representing the Hazelton Group in the Scottie gold mine-McTagg-Treaty area, southern Iskut River region. Numbers reference sources for fossil and radiometric ages. **1.** Norian-Rhaetian boundary (Wotzlaw et al., 2014); **2.** Rhaetian-Hettangian boundary (Schaltegger et al., 2008); **3.** Hettangian-Sinemurian boundary (Schaltegger et al., 2008); **4.** Cohen et al., (2013); **5.** ca. 214.2 Ma, 211.9 Ma, 201.0 Ma, and 190.6 Ma U-Pb zircon (this study); **6.** biochronologic and geochronologic compilations of Lewis (2013) based on Nadaraju (1993) and Nadaraju and Lewis (2001). **7.** Pleinsbachian ammonite fossil mold (this study) **8.** ca. 197 Ma, U-Pb zircon (Nelson, et al., 2021); **9.** MacDonald (1993) and Greig (2013); **10.** 198-189 Ma U-Pb zircon (Febbo et al., 2019); **11.** ca. 186 Ma youngest detrital zircon population (Nelson et al., 2021); **12.** Cutts et al. (2015); **13.** ca. 200.5 Ma U-Pb zircon (van Straaten et al., 2014); **14.** ca.190.6 Ma U-Pb zircon (Lepore, 2006); **15.** ca. 192.8 Ma U-Pb zircon (Alldrick, 1993).

the Jack Formation is sharp and ranges from paraconformable to unconformable. It represents an abrupt transition from siliclastic sedimentation to predominantly andesitic pyroclastic volcanism and epiclastic sedimentation (Nelson et al., 2018). Uranium-lead ages place the base of the Betty Creek Formation in the mid-Sinemurian (ca. 197 Ma), slightly younger than the youngest Jack Formation, indicating an abrupt onset of andesitic volcanism (Nelson et al., 2018). The Betty Creek Formation has been divided into three lithologically based, informal units (Fig. 2; Nelson et al., 2018). The Unuk River andesite unit is the most widespread and voluminous, extending from the Stewart mining camp into the McTagg area and west into the lower Iskut region. The Johnny Mountain dacite unit (ca. 194 Ma, Lewis, 2013) only occurs on Johnny Mountain (Fig. 1), and the Brucejack Lake felsic unit (ca. 185-178 Ma; Lewis, 2013) only occurs in the Brucejack area east of the McTagg anticlinorium. They represent local felsic centres within a regional andesitic volcanic field.

3. Previous work in the Stewart mining camp

Because of its accessibility from tidewater, the earliest mineral prospecting and small-scale mining in what would become known as the Golden Triangle began in the Stewart area in the early 1900s (Alldrick, 1993). By the 1980s, significant epithermal gold resources were identified at Scottie Gold (BC MINFILE 104B 034), Premier (BC MINFILE 104B 054), and adjacent Big Missouri (BC MINFILE 105B 045, 46). Scottie Gold was mined between 1981 and 1984, producing 2.98 million grams of gold and 1.63 million grams of silver. Premier was mined between 1989 and 1996; Big Missouri 1927-1942 and briefly 1988-89.

Geological mapping of the Stewart mining camp was conducted in the 1980s during the peak phase of mining and exploration activity (Alldrick, 1993). This work assigned all volcano-sedimentary units in the Stewart area to the Hazelton Group, in ascending order: alternating intermediate green volcanic and marine sedimentary beds of the Unuk River Formation; maroon and green volcanoclastic strata of the Betty Creek Formation; and dacitic tuffs of the Mt. Dilworth Formation (Alldrick, 1993). No Stuhini Group strata were recognized. The Unuk River Formation was subdivided into six members, in ascending order: lower andesite, lower siltstone, middle andesite, upper siltstone, upper andesite, and plagioclase-potassium feldspar-hornblende crystal-lithic tuffs and flows of the Premier porphyry member (Alldrick, 1993). The base of the overlying Betty Creek Formation was primarily defined by a change of colour in the andesitic volcanoclastic rocks from dark green to maroon and green (Alldrick, 1993).

Later workers pointed out that no clear, regionally applicable lithologic distinction exists between the Betty Creek and Unuk River formations, and that the variation of rock colouring records diagenesis, and occurs at all stratigraphic levels in the andesitic sequence (Lewis et al., 2001). Currently, all volcanic rocks in the lower Hazelton Group between Stewart and the Iskut River are included in the Betty Creek Formation (Lewis,

2013; Nelson et al., 2018). The andesitic volcanic and epiclastic sequences in the Stewart mining camp belong to the informal Unuk River andesite unit of the Betty Creek Formation (Lewis, 2013). The siltstone members of Alldrick (1993) were not addressed, because they do not occur in Betty Creek sections in the McTagg area where the revised stratigraphic schema was developed. The Mt. Dilworth Formation, which overlies the Betty Creek Formation, is Middle Jurassic (Cutts et al., 2015) and is part of the upper Hazelton Group (Gagnon et al., 2012).

4. Supracrustal rocks in the Scottie area: Stuhini and Hazelton groups

4.1. Stuhini Group

In the study area, the lowest Stuhini Group unit exposed consists of interlayered argillite, limestone, plagioclase-rich fine-grained sandstones, and felsic tuffs (Fig. 3); the base of this unit has not been observed. It grades up-section into an upper unit of alkalic volcanic breccias, flows and tuffs.

4.1.1. Lower fine-grained sedimentary-tuff unit

The lowest Stuhini Group unit in the study area outcrops along a 4 km-long ridge south of August mountain, and in a discontinuous belt extending north from the Lost Railway area (Fig. 3). It consists of dark grey, carbonaceous argillite with lesser light-toned, plagioclase-rich fine-grained sandstone, very fine grained felsic tuff interbeds, and discontinuous grey limestone lozenges up to 10s of m long (Fig. 4a). In some exposures, these rock types are interlayered on a cm to m scale. Sodium cobaltinitrite staining of a sample from a 2 m-thick sandstone bed indicates a low content of potassium feldspar (Fig. 4b). The sandstone contains angular to subangular grains of plagioclase (45%), quartz (20%), potassium feldspar (15%), and lesser relict mafic grains (Fig. 4c).

In the Domino area (Fig. 3), fine-grained dark grey argillites are interbedded with volcanic breccias and flows of the upper volcanic unit. These interbeds decrease in number and disappear up-section at the expense of purely volcanic beds, indicating a transitional contact with respect to the upper volcanic unit.

4.1.2. Upper volcanic unit

Alkalic volcanic and volcanoclastic deposits of this unit form a north-northwest trending belt extending from the eastern slopes of August mountain through Summit Mountain and continuing to the Domino area, in part covered by glaciers (Fig. 3). In this belt, light-toned augite-phyric trachyandesite-(latite)breccias, flows and flow-breccias, felsic flows, and lapilli tuffs interfinger with laminated felsic (trachyte) crystal lithic tuffs (Fig. 5; McPhie, 1993). Breccias of this unit overlie dark-toned argillaceous strata of the lower fine-grained sedimentary-tuff unit near the southern Berendon Glacier fork and east of August mountain (Fig. 3). The coarse-grained volcanoclastic units are typically monomictic, consisting of lapilli to bomb fragments embedded in a finely comminuted matrix of the same composition (Fig. 5a). Large, well-formed, fresh augite phenocrysts are abundant in the clasts. Less common polymictic

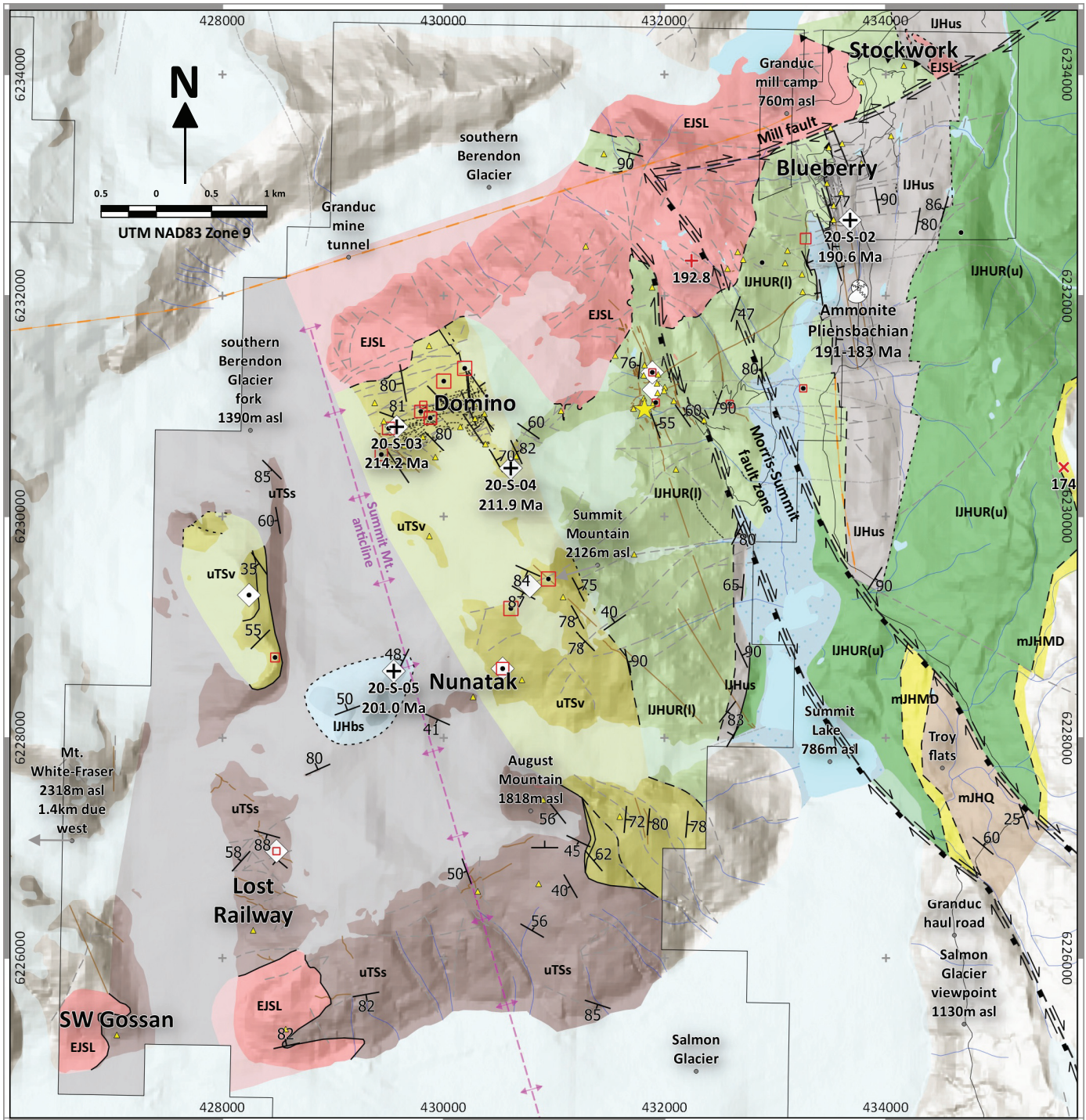


Fig. 3. Geology of the Scottie gold mine area.

varieties contain subangular to subrounded fragments of similar composition to the matrix but with a range of volcanic and hypabyssal textures. Some contain clasts of argillite and lesser chert, which may represent scavenged colluvial fragments. A set of 12 samples from this unit show a strong response to sodium cobaltinitrite staining, indicating high potassium feldspar and compositions in the field of trachyandesite (latite, based on subequal percentages of plagioclase and potassium

feldspar; Lemaître et al., 2002) and possibly trachyte (Figs. 3, 5b). Potassium feldspar, probably sanidine, forms very fine-grained aggregates along with variable amounts of plagioclase as igneous matrix to breccia and tuff clasts.

A crystal-lithic tuff bed near the base of the unit (20-S-03, Fig. 3) shows graded bedding and cross bedding that indicate younging towards the northeast (to top of photo Fig. 5c). The bed contains angular potassium-feldspar-rich lithic fragments

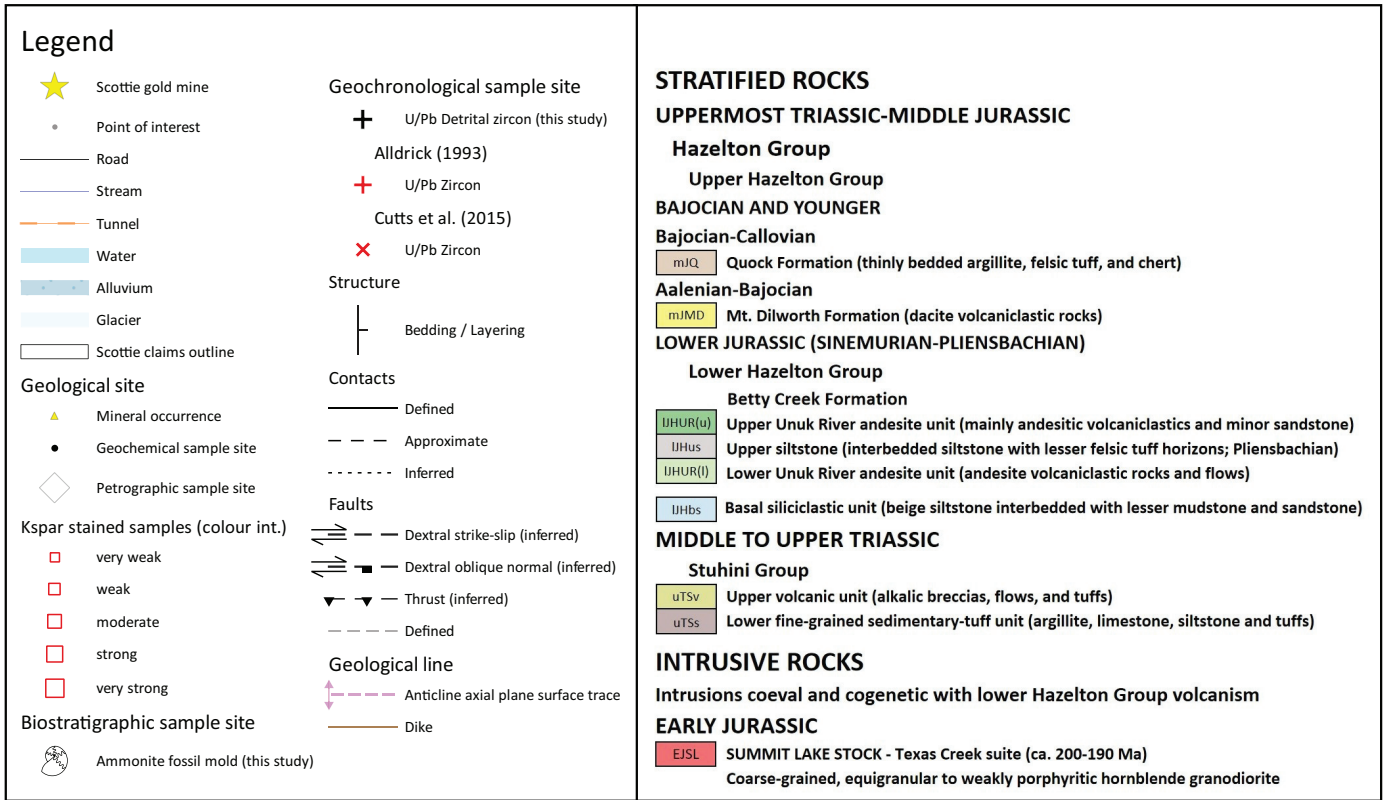


Fig. 3. Continued. Legend.

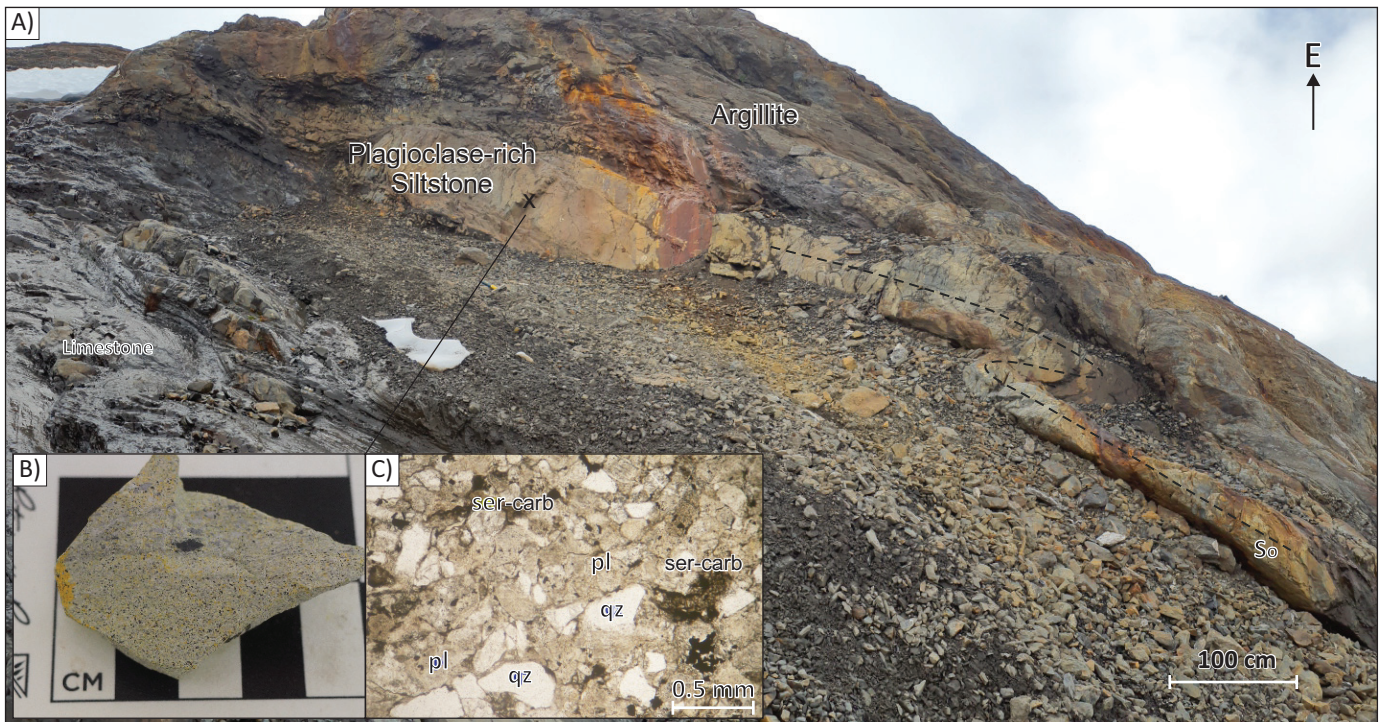


Fig. 4. Stuhini Group lower fine-grained sedimentary-tuff unit in the Lost Railway area (UTM 428488E, 6226977N). **a)** Interbedded argillite, with a prominent plagioclase-rich, fine-grained sandstone bed, and limestone. South-vergent tight fold in sandstone. **b)** Sodium cobaltinitrite stained fine-grained sandstone, showing weak response. **c)** Photomicrograph of plagioclase-rich, fine-grained sandstone, plane-polarized light. Small patches of secondary sericite and carbonate. pl = plagioclase; qz = quartz; ser-carb = sericite + carbonate.

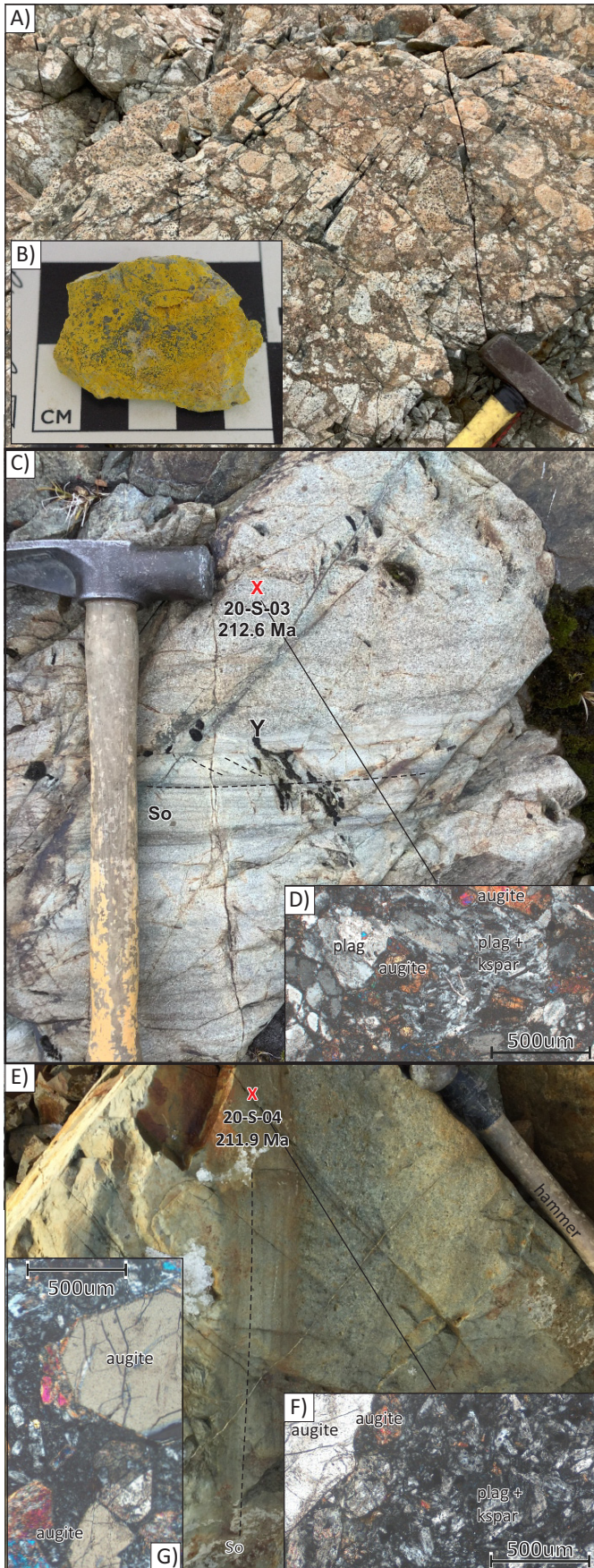


Fig. 5. Stuhini Group, augite-bearing alkalic volcanic rocks of upper volcanic unit. **a)** Matrix-supported latite volcanic breccia, north of Domino area (UTM 430001E, 6231228N). **b)** Sodium cobaltinitrite-stained hand sample of breccia in a) indicates abundant matrix potassium feldspar. **c)** Interbedded beige parallel- and cross-stratified latite crystal-lithic tuff and lapilli tuff. U-Pb detrital zircon LA-ICPMS sample site 20-S-03 (UTM 429535E, 6230888N). MDA = 214.2 ± 1.0 Ma (see below). **d)** Photomicrograph displays augite-plagioclase-phyric lithic fragment with potassium- and plagioclase feldspar-rich matrix. Crossed polarizers. **e)** Interval of laminated augite-rich crystal-lithic tuffs interbedded with lapilli tuff. U-Pb detrital zircon LA-ICPMS sample site 20-S-04 (UTM 430607E, 6230437N); U-Pb crystallization age = 211.9 ± 3.6 Ma (see below). **f)** Photomicrograph of fragment from laminated tuff displays large, embayed augite phenocryst in plagioclase-rich matrix with interstitial potassium feldspar. Crossed polarizers. **g)** Large, fresh euhedral and broken augite phenocrysts. Crossed polarizers. aug = augite, plag = plagioclase, Kspar = potassium feldspar.

(50%), broken plagioclase (20%), and augite (5%) crystal clasts (Fig. 5d). Although compositionally similar, lithic clasts in this tuff exhibit a wide range of igneous textures, from holocrystalline with well-formed matrix plagioclase and interstitial potassium feldspar (Fig. 5d) to nearly aphanitic. The top of the volcanic unit is marked by very coarse, light-toned augite-phyric volcanoclastic rocks (Figs. 5a, b, e, f). A crystal-lithic tuff interbedded with lapilli tuff (Fig. 5e; 20-S-4, Fig. 3) contains densely packed augite-phyric plagioclase-rich lithic fragments (Fig. 5f) and euhedral to broken, fresh augite phenocrysts (Fig. 5g), with a few dark green-pleochroic hornblende crystal clasts. Plagioclase does not form phenocrysts in this sample. Lithic clasts are all augite-phyric, but show different matrix textures ranging from felted plagioclase and anhedral interstitial potassium feldspar (Fig. 5f), to nearly glassy. Some augite crystals in the igneous matrix show embayed margins (Fig. 5f) that may reflect partial resorption by the melt.

4.2. Lower Hazelton Group

A nunatak in the west-central part of the map area forms an isolated exposure of basal Hazelton Group siltstone, sandstone, and mudstone, surrounded by Stuhini Group strata (Fig. 3). The eastern half of the map area is underlain by a thick, east-younging section of the Betty Creek Formation of the lower Hazelton Group. The section there comprises two units of feldspar-hornblende-phyric andesitic flows, tuffs, breccias, and conglomerates assigned to the Unuk River andesite unit of the Betty Creek Formation, following the lithologically based usage of Nelson et al. (2018), and an intervening siltstone unit (Figs. 2, 3). Siltstones have not been previously recognized as components of the Betty Creek Formation (Lewis, 2013, Nelson et al., 2018). Alldrick (1993) included the siltstone in the Unuk River Formation; however subsequent workers have restricted the term ‘Unuk River’ to denote andesitic lithofacies within the Betty Creek Formation (Lewis, 2013; Nelson et al., 2018). In this report we assign it the informal name of ‘upper siltstone unit’, based on its assigned name in Alldrick (1993).

East of the map area, the Betty Creek Formation is overlain by felsic tuffs of the Mount Dilworth Formation (upper Hazelton Group, Middle Jurassic), west of Troy flats and along the flanks of the north trending Mount Shorty-Stevenson ridgeline (Figs. 1-3; Alldrick, 1993).

4.2.1. Basal siliciclastic rocks

West of Nunatak (Fig. 3), the lowermost Hazelton unit forms an outlier surrounded by the lower fine-grained sedimentary-tuff unit of the Stuhini Group and extensively covered by glaciers. The outlier consists of beige siltstone with lesser interbeds of sandstone and mudstone (Fig. 6). The siltstone consists of sericite-altered plagioclase grains with subordinate subrounded to subangular quartz grains (Fig. 6b). Because the upper volcanic unit of the Stuhini Group is missing, the glacier-covered basal contact of this siliclastic unit may record the regionally developed sub-Hazelton Group unconformity.

4.2.2. Betty Creek Formation

4.2.2.1. Lower Unuk River andesite unit

A thick andesitic succession overlies the upper Stuhini Group volcanic unit on the eastern slope of Summit Mountain, extending into the Blueberry area (Fig. 3). It consists predominantly of matrix-supported plagioclase-hornblende-phyric andesite breccias and flows, with little or no matrix potassium feldspar (Fig. 7). Coherent and volcanoclastic eruptive units interfinger and grade into one another at outcrop scale. Volcanic breccias typically contain lapilli to bomb fragments (Figs. 7a, c) of similar composition to the matrix. Clasts are angular and irregular. Fragments of augite-phyric latite and argillite occur locally. Rare pyroxene phenocrysts are much smaller than those in the underlying upper Stuhini volcanic unit. Generally, layering in this unit appears subparallel to its lower contact and with layering in subjacent rocks of the upper Stuhini Group volcanic unit. We interpret this contact as a paraconformity.

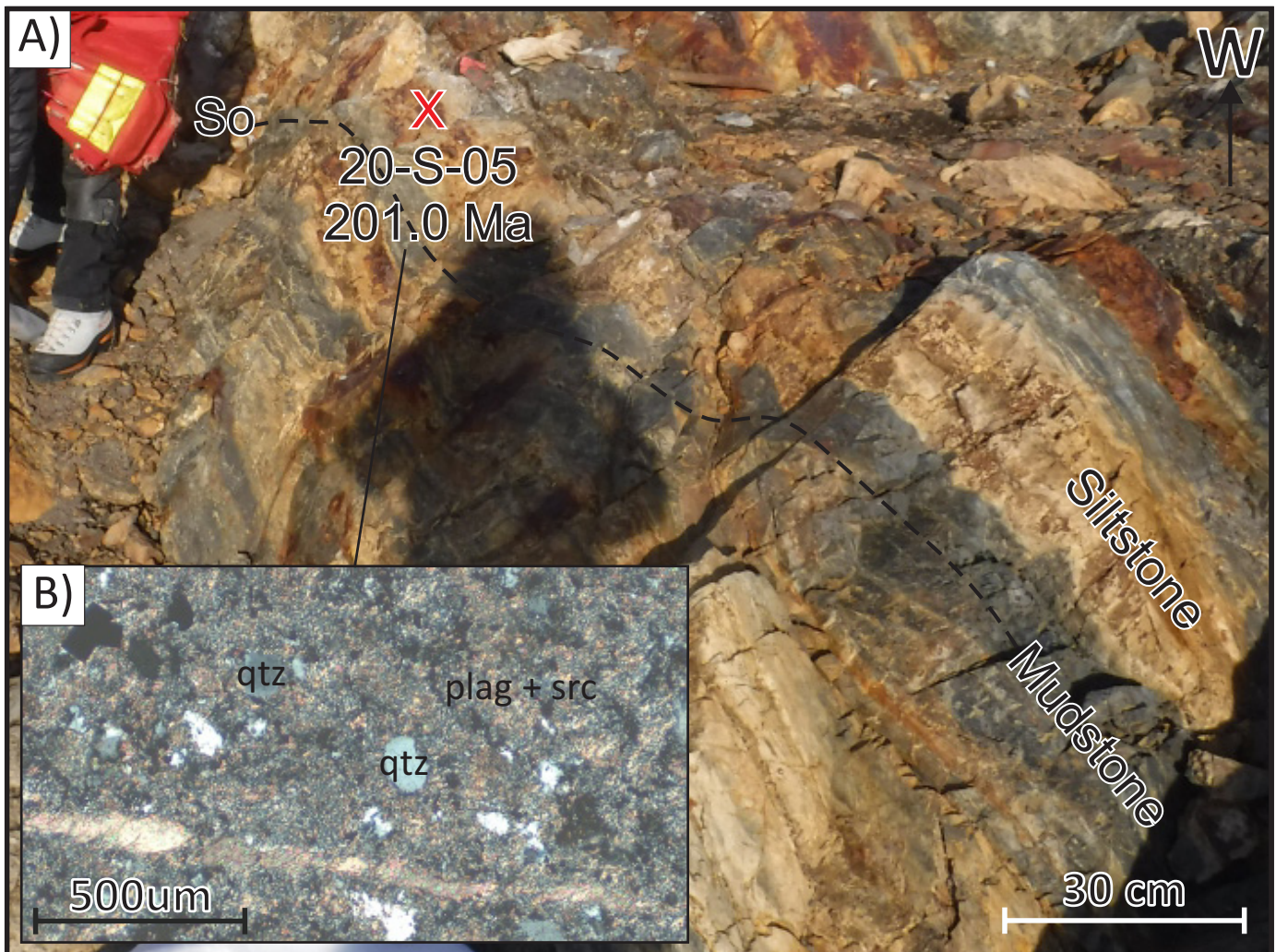


Fig. 6. Lower Hazelton Group, basal siliciclastic rocks. **a)** Siltstone and mudstone beds; U-Pb detrital zircon sample site 20-S-5, west of Nunatak area (UTM 429549E, 6228603N). MDA = 201.0 ± 5.2 Ma (see below). **b)** Photomicrograph of sample 20-S-5 displays mainly heavily sericitized detrital plagioclase grains with scattered angular to subrounded quartz. Crossed polarizers. Qtz = quartz, plag + src = sericite-altered plagioclase.



Fig. 7. Lower Hazelton Group, Betty Creek Formation, lower Unuk River unit andesites. **a)** Monomictic, matrix-supported, hornblende-phyric andesitic volcanic breccia, 1.4 km east of the Scottie gold mine area (UTM 433255E, 6231163N). **b)** Breccia matrix hand sample very weakly stained by sodium cobaltinitrite. **c)** Monomictic matrix-supported andesite volcanic breccia from 1 km east of the Scottie gold mine area (UTM 432881E, 6231341N). **d)** Weakly sericite altered, hornblende-phyric andesite flow from the Scottie gold mine area (UTM 431923E, 6231034N). **e)** Very weakly sodium cobaltinitrite-stained hand sample of flow in d).

4.2.2.2. Upper siltstone unit

Grey feldspar-rich siltstones outcrop in a north-striking, northerly thickening sequence east of and stratigraphically above the lower Unuk River andesite unit (Figs. 3, 8). These strata have sub-vertical dips and contain mud rip-up clasts, flame structures, load casts, and graded- and cross-bedding structures that consistently indicate younging to the east. A sample from this unit (Fig. 8b) contains subangular grains of potassium feldspar (30%), fine-grained potassium feldspar-rich lithic grains (20%), plagioclase (25%), and quartz (5%). Carbonate minerals (5%) occur as patches in the matrix. Towards the upper half of the siltstone unit, thin (<5 m), internally-laminated felsic ash tuff beds interfinger with siltstone beds.

In its southernmost exposure west of Summit Lake, the unit is approximately 130 m thick (Fig. 3), whereas at its northern extent in the Blueberry area 6 km along strike, it may be as much as 1200 m thick. The upper contact with andesites of the upper Unuk River unit lies under Quaternary cover. An ammonite fossil mold has been tentatively assigned a Pliensbachian age (M. Golding, personal communication 2021, based on identification by Terry Poulton).

4.2.2.3. Upper Unuk River andesite unit

Light to dark green and maroon andesitic breccias and tuffs overlie the upper siltstone unit on the eastern side of the map area (Figs. 3, 9). Small hornblende and plagioclase phenocrysts are common in this unit. Most breccias are monomictic and

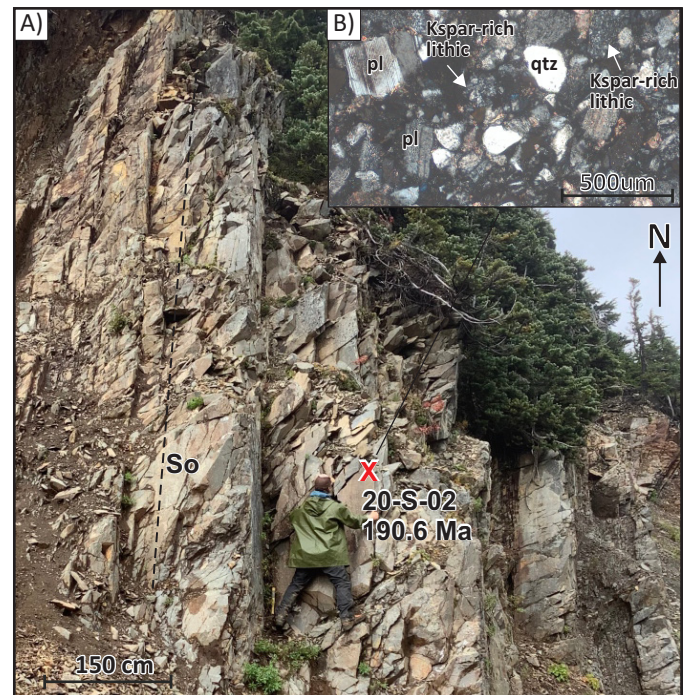


Fig. 8. **a)** Lower Hazelton Group, Betty Creek Formation, upper siltstone unit and U-Pb detrital zircon sample site 20-S-2 from the Blueberry area (UTM 433678E, 6232684N). MDA = 190.6 ± 1.7 Ma (see below). **b)** Photomicrograph of sample 20-S-2, illustrating abundant feldspar and sparse quartz. Kspar = potassium feldspar, plag = plagioclase, qtz = quartz.



Fig. 9. Upper Unuk River unit andesites. **a)** Matrix-supported green and maroon volcanic breccia, 1.3 km east-southeast of the Blueberry area (UTM 434680E, 6232572N). **b)** Maroon matrix-supported volcanic breccia with feldspar-phyric clasts, 1.5 km east-southeast of the Blueberry area (UTM 434793E, 6232514N).

matrix-supported (Figs. 9a, b); locally, apparent long axes align to define a crude layering (Fig. 9a). In some breccias, angular lapilli to bomb fragments of laminated felsic tuff are similar in colour and texture to felsic volcanic interbeds in the upper siltstone unit to the west, and are interpreted as accidental clasts derived from them. The andesitic sequence contains minor sandstone interbeds with mud rip-up clasts; cross-bedding and graded bedding indicate younging to the east.

5. Intrusive rocks: Summit Lake stock, Texas Creek plutonic suite

Within the Stewart mining camp, the Texas Creek plutonic suite (ca. 202-190 Ma) consists of the Texas Creek batholith, the Summit Lake stock, Premier porphyry dikes, and a variety of related dikes and sills (Alldrick, 1993; Anderson, 1993). The Texas Creek batholith and Premier porphyry dikes outcrop 10 km south of the study area, near the past-producing Premier mine (Fig. 1). There, gold-silver mineralization and associated

alteration zoning patterns are spatially related to plutons of the Texas Creek suite and Premier porphyry dikes (Bird et al., 2020). Major element analysis of the Summit Lake stock, Texas Creek batholith, and Premier porphyry dikes indicates that the suite is subalkaline, calc-alkaline in composition with elevated potassium contents (Alldrick, 1993). Discriminant diagrams also show that Texas Creek intrusions are chemically similar to, and likely comagmatic with, Hazelton Group volcanic rocks (Alldrick, 1993).

The Summit Lake stock outcrops as an elongate northeast trending (~7 km long) body at the northern extent of the study area (Fig. 3). It consists of medium- to coarse-grained equigranular to porphyritic potassium-feldspar and hornblende granodiorite to tonalite (Alldrick, 1993). Less common weakly foliated, mafic enclave-bearing phases are interpreted as older phases of the stock (Alldrick, 1993). The stock cuts across northwest-trending strata of the upper volcanic unit of the Stuhini Group and the lower Unuk River andesite unit. Northeast of the main stock, a small, probably related body cuts the upper siltstone unit (Fig. 3).

Regionally, U-Pb ages of Texas Creek suite intermediate porphyritic intrusions (Mitchell suite at KSM and Lehto suite in the Snippaker area; Fig. 1) are coeval with Unuk River unit andesites (Fig. 2; Febbo et al., 2015; Kyba and Nelson, 2015; Febbo, 2016; Nelson et al., 2018). In the Scottie area, the stock returned a 192.8 ± 2 Ma U-Pb age (Fig. 2; Alldrick, 1993). North of the study area, on the Tennyson claims, an early Texas Creek suite intrusion yielded a U-Pb zircon age of 200.5 ± 0.8 Ma (van Straaten et al., 2014), and a dike is 190.6 ± 1.3 Ma (LA-ICP-MS U-Pb zircon, Lepore, 2006).

6. Structural geology

The main structural element in the map area is a regional-scale fold, the Summit Mountain anticline, which is cored by Stuhini Group rocks (Fig. 3). The anticline trends north-northwest and is asymmetric, verging to the east-northeast. It displays a subvertical to steeply east-dipping eastern limb of eastward-younging Hazelton Group rocks and a moderately southwest-dipping western limb defined by Hazelton Group units that cap the Mt. White-Fraser ridgeline, 2 km west of the study area. This major fold forms an anticline-syncline pair with the Mount Dilworth syncline farther east (Alldrick, 1993). These structures are first-order features of the Early Cretaceous Skeena fold and thrust belt (Evenchick, 2001).

Two northwest-trending, west-side down dextral-oblique normal faults (Morris-Summit fault zone) extend from the southeast corner of the map area and appear to cut the Summit Lake stock. In the northeast corner of the map area, the Mill fault, a major east-northeast-trending dextral strike-slip structure, also appears to cut the Summit Lake stock. Stuhini and Hazelton group strata are also cut by relatively minor northwest- and east-trending cross faults (Fig. 3).

7. Geochemistry

Eighteen representative samples from volcanic-volcaniclastic

units were collected across the study area for whole-rock geochemical analysis. Twelve samples were collected from the upper Stuhini volcanic unit, five samples from the lower Unuk River andesite unit and one sample from the upper Unuk River andesite unit (Table 1; sample locations on Fig. 3). During sample collection every effort was taken to avoid altered rock. A diamond saw was used to trim and remove veins and to minimize weathering. Major elements for most samples were analyzed at Australian Laboratory Services (ALS; Terrace, BC, laboratory) using ICP-Atomic emission spectrometric methods; two samples were analyzed at Société Générale de Surveillance (SGS; Burnaby, BC, laboratory) using ICP-optical emission spectrometric methods; in each case following lithium metaborate fusion and nitric acid digestion. The summary of major element geochemical results in Table 1 shows total weight percent values (between 91.2 and 101.6 wt.%) and loss on ignition values (between 1.8 and 5.6 wt.%). Full analytical datasets and background information are presented in Stanley and Nelson (2022).

7.1. Results

7.1.1. Upper volcanic unit, Stuhini Group

In the field, rocks of the upper volcanic unit appear as mainly large-augite-phyric trachyandesite (latite) to aphyric trachyte volcanic breccias, flows, and tuffs (Fig. 5). All twelve samples plot in the alkaline field, ranging from basaltic trachy-andesite, trachy-andesite, phono-tephrite, tephri-phonolite, to phonolite compositions on the total alkali versus silica discrimination diagram (TAS; Fig. 10a), and all samples, except D707510 and D707513, plot within the shoshonite series, ranging from absarokite, shoshonite, to banakite compositions on the potassium versus silica discrimination diagram (Fig. 10b). The abundance of augite phenocrysts in most of these rocks may skew the analytical compositions to lower silica contents and lead to clustering in the basaltic trachy-andesite field as opposed to their field identification as predominantly latites. Lemaitre et al. (2002) noted that the TAS diagram is intended as an interpretive tool for aphanitic volcanic rocks because crystal accumulation may produce spurious results. For this reason, field classification of these rocks should take precedence. Their highly potassic, shoshonitic geochemical character agrees with field identification of abundant igneous potassium feldspar.

7.1.2. Unuk River andesite unit, Hazelton Group

The Unuk River andesite unit consists mainly of matrix-supported feldspar-hornblende-phyric andesite breccias and less common coherent andesites interpreted as flows. The augite phenocrysts in this unit are subordinate to plagioclase and hornblende and are smaller than those in the upper volcanic unit of the Stuhini Group. Four samples plot within the alkaline field (basaltic trachy-andesite) adjacent the subalkaline boundary, and two plot within the subalkaline field (basalt and basaltic trachy-andesite) of the TAS discrimination diagram (Fig. 10a). On the K_2O vs. SiO_2 diagram, two samples plot within the shoshonite series (range from absarokite-shoshonite), two in

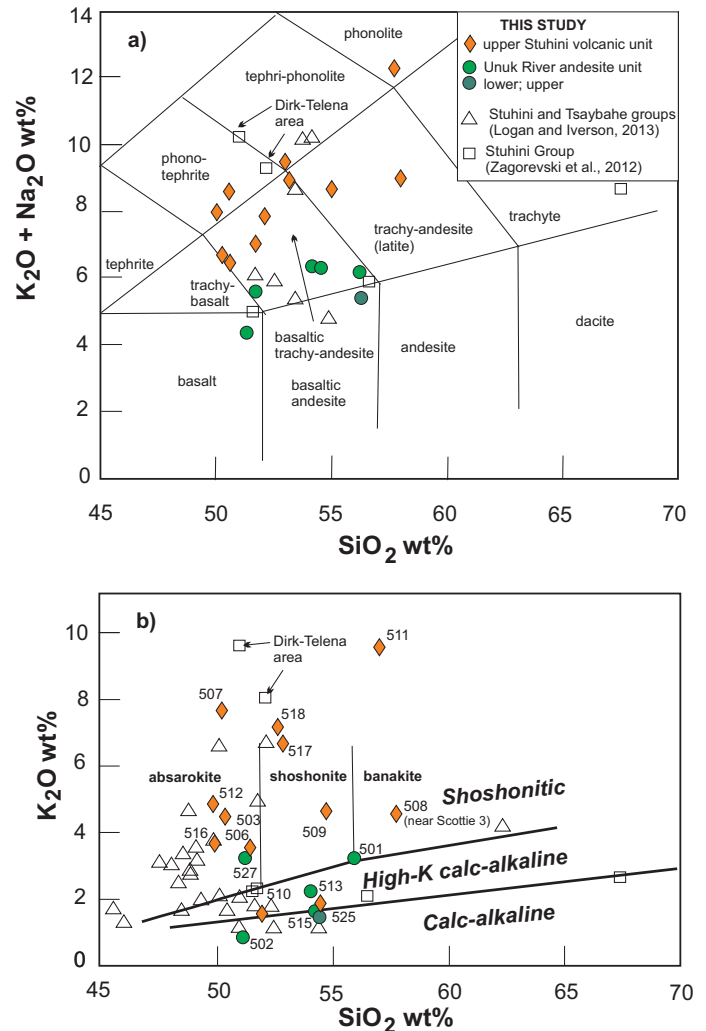


Fig. 10. a) Total alkalis vs. silica (Le Bas et al., 1986) rock type discrimination plot. Alkaline and subalkaline/tholeiitic fields after Irvine and Baragar (1971). Values are recalculated from Table 2 data to account for loss on ignition (e.g., $SiO_2 * 100 / (Total-Loss \text{ on ignition})$). **b)** Classification plot based on SiO_2 vs. K_2O (after Peccerillo and Taylor, 1976; Morrison, 1980), used to distinguish shoshonitic, high-K calc-alkaline, calc-alkaline and tholeiitic series rocks. Values are recalculated from Table 2 data to account for loss on ignition (e.g., $SiO_2 * 100 / (Total-Loss \text{ on ignition})$). Legend as in a).

the high potassium calc-alkaline series, and two in the calc-alkaline series (Fig. 10b).

8. Detrital zircon geochronology

We collected four samples for laser ablation-inductively coupled plasma-mass spectrometry (LA-ICP-MS) analysis: two from the upper alkalic volcanic unit of the Stuhini Group; one from the basal siliciclastic unit of the Hazelton Group; and one from the upper siltstone unit, Betty Creek Formation (Table 2). The analyses were carried out at the Pacific Centre for Isotopic and Geochemical Research (PCIQR), University of British Columbia, using a Resonetics RESolution M-50-LR. The full analytical details, complete dataset, and data processing methods are presented in Stanley and Nelson (2022).

Table 1. Whole rock geochemical results from the Scottie gold mine area. All locations are NAD 83 Zone 9; samples D707527 and D707525 were analyzed at SGS Laboratories, all others were analyzed at ALS laboratories.

Sample	D707503	D707506	D707507	D707508	D707509	D707510	D707511	D707512	D707513
Group	Stuhini	Stuhini	Stuhini	Stuhini	Stuhini	Stuhini	Stuhini	Stuhini	Stuhini
Unit	upper volcanic unit	upper volcanic unit	upper volcanic unit	upper volcanic unit	upper volcanic unit	upper volcanic unit	upper volcanic unit	upper volcanic unit	upper volcanic unit
Rock Type	Augite-phyric latite breccia	Augite-phyric latite breccia	Augite-phyric latite breccia	Latite tuff	Trachyte	Felsic tuff	Felsic tuff	Latite	Latite
Easting	430190	429794	430001	429503	429437	429881	429879	428240	428476
Northing	6231344	6230954	6231228	6230801	6230560	6230893	6230895	6229290	6228726
SiO₂ (wt.%)	48.1	50.8	46.7	57.2	53.6	47.3	56.7	48.3	51.8
Al₂O₃ (wt.%)	15.35	16.8	15.2	17.1	17.1	17.15	19.25	17.4	17.1
Fe₂O₃ (wt.%)	10.3	9.15	8.76	6.24	8.36	9.21	6.55	9.56	10.2
CaO (wt.%)	8.75	5.71	7.3	4.32	4.28	5.2	1.07	6.36	4.15
MgO (wt.%)	5.19	7.72	5.17	3.88	4.04	3.24	1.87	6.07	4.25
Na₂O (wt.%)	1.94	3.41	0.86	4.38	3.88	5.78	2.54	3.03	4.25
K₂O (wt.%)	4.34	3.58	7.19	4.56	4.57	1.44	9.6	4.8	1.79
TiO₂ (wt.%)	0.88	0.76	0.67	0.74	1.04	0.75	0.6	0.74	0.9
MnO (wt.%)	0.21	0.18	0.21	0.1	0.21	0.21	0.14	0.18	0.18
P₂O₅ (wt.%)	0.36	0.31	0.38	0.28	0.41	0.6	0.2	0.31	0.36
LOI	2.4	2.86	4.29	2.26	2.43	4.26	1.75	4.18	4.96
Total	98.07	101.62	97.25	101.45	100.33	95.44	101.29	101.24	100.23

From each sample, 79 grains were hand-picked and mounted for analysis, except for 20-S-4, which yielded only three zircon grains. Probability density and histogram plots of detrital zircon ages were generated using the Isoplot 3.70 and 4.15 add-in for Microsoft Excel (Ludwig, 2008). Maximum Depositional Ages (MDA) were assigned based on Youngest Statistical Populations (YSP), according to the method of Coutts et al. (2019). To identify multiple source populations, we applied the Unmix routine in Isoplot 3.70 (Ludwig, 2008).

8.1. Stuhini Group, upper volcanic unit, samples 20-S-3 and 20-S-4

Sample 20-S-3 is of an interbedded latite crystal tuff and lapilli

tuff 500 m west of the Domino area, near the interpreted base of the unit (Figs. 3, 5c). The main peak in the probability plot is ca. 219 Ma, with a younger shoulder at ca. 214 Ma (Fig. 11a, Table 2). It also contains a single Paleozoic grain, ca. 381.5 Ma (Stanley and Nelson, 2021). Although the youngest grain is 204.9 ± 4.7 Ma, it is highly discordant (9.4%) and we attribute its young age to lead loss. The Youngest Statistical Population has a weighted average of 214.2 ± 1.0 Ma based on 27 grains (Fig. 11b). We interpret this as the crystallization age of the tuff. The prominent older peak (ca. 219 Ma) is attributed to recycling of older Stuhini Group and Stikine plutonic suite zircons.

Sample 20-S-4 is of an augite-phyric latite crystal-lithic lithic

Table 1. Continued.

Sample	D707516	D707517	D707518	D707501	D707502	D707504	D707515	D707527	D707525
Group	Stuhini	Stuhini	Stuhini	Hazelton	Hazelton	Hazelton	Hazelton	Hazelton	Hazelton
Unit	upper volcanic unit	upper volcanic unit	upper volcanic unit	lower Unuk River andesite	lower Unuk River andesite	lower Unuk River andesite	lower Unuk River andesite	lower Unuk River andesite	upper Unuk River andesite
Rock Type	Augite-phyric trachyte breccia	Augite-phyric crystal tuff	Latite tuff	Hbl-phyric andesite breccia	Hbl-phyric andesite	Andesite breccia	Hbl-plag-phyric dacite	Hbl-Fsp-phyric andesite	Andesite
Easting	430534	430608	430947	432590	431923	433255	431891	432883	434680
Northing	6228626	6229168	6229436	6231022	6231034	6231163	6231307	6232300	6232572
SiO₂ (wt.%)	48	50.6	45.6	55.1	48.5	47.9	53	51.18	54.36
Al₂O₃ (wt.%)	16.2	16	16.4	16.6	14.9	14.95	16.2	16.43	18.26
Fe₂O₃ (wt.%)	9.56	8.86	7.48	9.39	12.15	9.51	4.32	10.65	8.55
CaO (wt.%)	5.54	5.26	3.14	5.56	7.7	4.35	11.3	8.41	6.05
MgO (wt.%)	8.92	4.86	4.24	4.2	5.83	4.78	5.21	5.46	3.04
Na₂O (wt.%)	2.93	2.11	1.95	2.82	3.31	3.63	4.6	2.34	3.84
K₂O (wt.%)	3.59	6.46	6.24	3.22	0.88	2.01	1.66	3.27	1.53
TiO₂ (wt.%)	0.74	0.76	0.63	0.81	0.85	0.72	0.77	0.79	0.69
MnO (wt.%)	0.13	0.17	0.13	0.19	0.2	0.17	0.11	0.11	0.22
P₂O₅ (wt.%)	0.3	0.39	0.46	0.28	0.37	0.37	0.41	0.44	0.32
LOI	2.79	2.61	4.52	2.22	3.74	4.12	2.47	1.98	5.63
Total	99.03	98.49	91.17	100.73	98.59	92.77	100.19	101.06	102.49

tuff from the top of the volcanic unit, north of Summit Mountain (Figs. 3, 5e). It only yielded three zircon grains, all of which are concordant (Fig. 11c). A weighted average of the youngest two grains is 211.9 ± 3.6 Ma (Table 2), which is tentatively considered the crystallization age of the tuff. Although based on sparse data, this age overlaps within error the more robust age derived from sample 20-S-3. Thus, alkalic volcanism at ca. 214 Ma was the last event recorded by the Stuhini Group in the Scottie area.

8.2. Lower Hazelton Group

8.2.1. Basal siliciclastic rocks, sample 20-S-5

Sample 20-S-5 is of a siltstone from west of the Nunatak area

(Figs. 3, 6). Zircon analyses show a main probability density peak of ca. 219 Ma, with subordinate peaks at ca. 201, 214, and 232 Ma (Fig. 12a). The Youngest Statistical Population of four grains has a weighted average age of 201.0 ± 5.2 Ma (Table 2), interpreted as the maximum depositional age. The older populations show input from main-stage Stuhini Group and Stikine suite sources and from the immediately underlying uppermost Stuhini Group volcanic unit.

8.2.2. Betty Creek Formation, upper siltstone unit, sample 20-S-2

Sample 20-S-2 is from a well-sorted potassium feldspar-rich siltstone bed in the Blueberry area (Figs. 3, 8a, b). Zircon

Table 2. Summary of results from LA-ICP-MS U-Pb zircon analysis for samples from Scottie gold mine area. All locations are NAD 83 Zone 9. N = Grains analyzed (total); N1 = Concordant grains (<10% discordant).

Sample ID	Unit	Easting	Northing	Description	N	N1	Youngest grain	Youngest Statistical Population	Probability density peaks	Umix ages (fractions)
20-S-3	Stuhini Group, upper volcanic unit	429535	6230888	Beige laminated latite crystal-lithic tuff. Kspar-rich, plagioclase + augite-phyrlic lithics; plagioclase and augite crystal clasts	78	65	204.9 ±4.7 Ma discordant; does not form coherent population with older grains	214.2 ±1.0 Ma (27 grains, except youngest; MSWD=0.89, prob=0.63); volcanic crystallization age	215 Ma 219 Ma 244 Ma	207.4 ±5.5 Ma (.04) 214.52 ±1.9 Ma (.36) 221.22 ±1.8 Ma (.45) 230.5 ±3.8 Ma (.14) 243.7 ±7.3 Ma (.02) relative misfit = 0.705
20-S-4	Stuhini Group, upper volcanic unit	430607	6230437	Laminated latite tuff with augite-phyrlic lithic clasts	3	3	211.9 ±3.6 Ma (youngest 2 of 3 total grains) volcanic crystallization age	n/a	n/a	n/a
20-S-5	Hazelton Group basal clastic unit	429549	6228603	Siltstone from mudstone-siltstone-fine sandstone sequence	79	67	198.5 ±4.7 Ma	201.0 ±5.2 Ma (4 grains, MSWD=0.16, prob=0.92) MDA	201 Ma 215 Ma 220 Ma 234 Ma	201.4 ±3.1 Ma (.06) 210.9 ±5.3 Ma (.16) 214.6 ±4.3 Ma (.31) 221.7 ±2 Ma (.38) 232.3 ±4.5 Ma (.09) relative misfit = 0.617
20-S-2	Hazelton Group, Betty Creek Fm., upper siltstone unit	433678	6232684	Light grey homogenous siltstone	79	76	189.7 ±3.7 Ma	190.6 ±1.7 Ma (youngest 4 grains, MSWD=0.104, prob=0.96) MDA	190.5 Ma 198-203 Ma 216 Ma 243 Ma	197.83 ±1.3 Ma (.20) 204.92 ±2.7 Ma (.23) 216.46 ±1.1 Ma (.47) 226.6 ±2.6 Ma (.10) relative misfit = 0.366

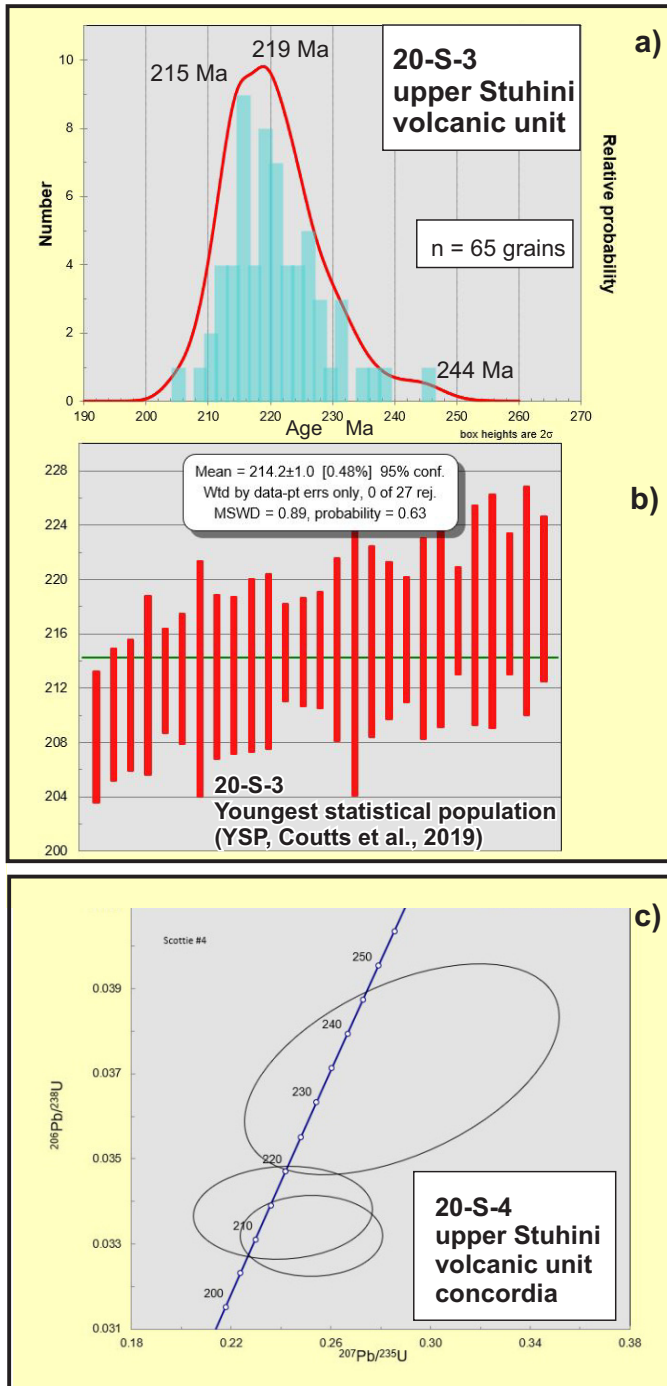


Fig. 11. Detrital zircon data for upper Stuhini Group alkalic volcanic unit. **a)** Probability density plot for 20-S-3. **b)** Weighted average for Youngest Statistical Population of 27 grains in sample 20-S-3. **c)** Concordia plot for 3 grains recovered from 20-S-4.

analyses display a prominent combined population density peak ca. 216–226 Ma, with lesser peaks ca. 190.5, 201, and 243 Ma (Fig. 12b). It also contains three Paleozoic grains with ages of 248.5, 283.1, and 317.5 Ma (Stanley and Nelson, 2021). The Youngest Statistical Population of four grains has a weighted average of 190.6 ± 1.7 Ma (Table 2), which we interpret to be the maximum depositional age for this unit. It agrees with

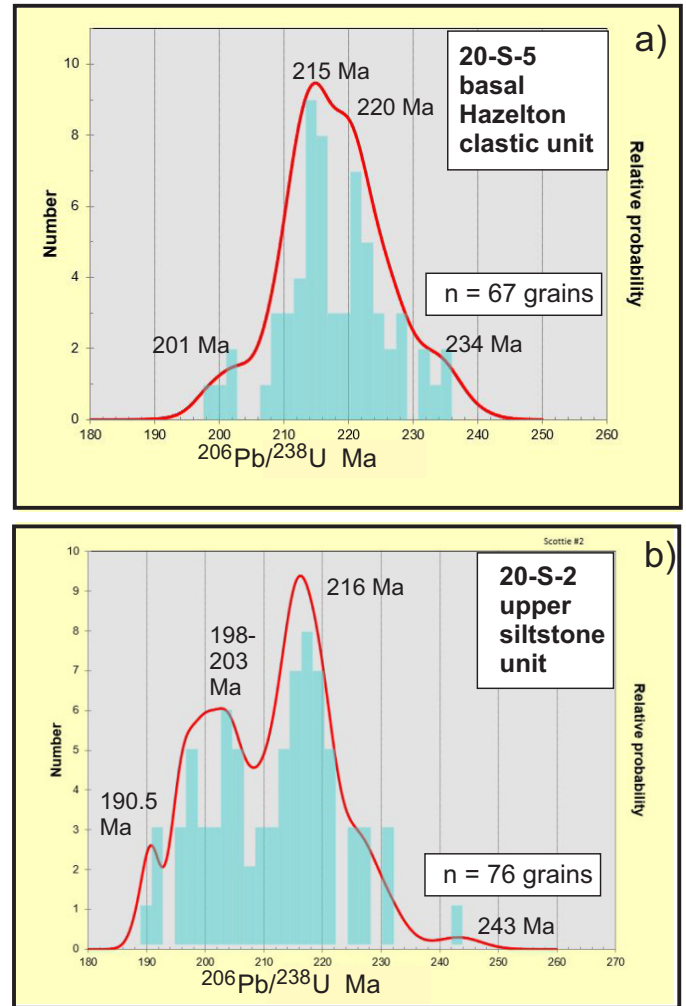


Fig. 12. Zircon age probability plots for lower Hazelton Group. **a)** Probability density plot for siltstone of basal siliciclastic unit. **b)** Probability density plot for upper siltstone unit, Betty Creek Formation.

the Pliensbachian age of enclosed ammonites. The prominent Late Triassic peak provides evidence for continued supply of detritus from Stuhini Group and Stikine suite sources in the Early Jurassic, likely derived from erosion of nearby uplifts.

9. Discussion

9.1. Revised stratigraphy of the Scottie gold mine area and Stewart mining camp

This study has shown that units belonging to the Stuhini Group are present in the Stewart mining camp, underlying previously recognized lower Hazelton Group strata (Alldrick, 1993). It presents a revision of Hazelton Group stratigraphic nomenclature for the Scottie area that aligns with current terminology for strata flanking the McTagg anticlinorium (Lewis, 2013; Nelson et al., 2018).

The lower fine-grained sedimentary-tuff unit of the Stuhini Group resembles argillite-siltstone-sandstone units in the core of the McTagg anticlinorium and near Granduc (Lewis, 2013). The upper volcanic unit gradationally overlies the dark-

coloured sedimentary strata, forming the highest stratigraphic level of the Stuhini Group in the Scottie area. The youngest zircon population from a crystal-lithic tuff near the base of the unit is 214.2 ± 1.0 Ma, or Late Norian.

Interbedded siltstone, sandstone and mudstone form the lowest Hazelton Group unit in the area. The basal contact of this unit with the underlying lower sedimentary-tuff unit of the Stuhini Group is covered. Because the upper Stuhini volcanic unit is missing at this locality the contact may be an unconformity. The maximum depositional age of the basal Hazelton unit (ca. 201 Ma) is close to the Triassic-Jurassic boundary (Cohen et al., 2013), similar in age to the Jack Formation (Hettangian-Sinemurian) in the McTagg anticlinorium (Fig. 2). Because the basal unit is much finer grained than the Jack Formation, it may be a distal equivalent. Notably, the unit is at least 10 m.y. younger than the upper volcanic unit of the Stuhini Group, indicating a significant hiatus between Stuhini and Hazelton deposition in the Scottie area.

The main section of the Hazelton Group overlies the upper volcanic unit of the Stuhini Group on the eastern limb of the Summit Mountain anticline. Eastward younging directions are observed in both units. Most of the contact is ice-covered or inaccessible. It is most likely paraconformable, given the >10 m.y. depositional hiatus between youngest Stuhini and oldest Hazelton units. All strata in the main Hazelton sequence are assigned to the Betty Creek Formation. The lower and upper andesite units belong to the lithologically defined Unuk River andesite unit. Lithological equivalents of the intervening siltstone unit do not occur in the McTagg area, where current Betty Creek stratigraphy has been defined (Lewis, 2013, Nelson et al., 2018). We refer to it informally as the “upper siltstone unit”, following Alldrick (1993). Future workers in the Stewart camp may choose to assign this lithofacies a topographically based name.

9.2. Regional significance of the upper volcanic unit, Stuhini Group

The upper volcanic unit is unusual because of its age (ca. 214 Ma) which is relatively young for the Stuhini Group (mainly Carnian-Norian faunal ages; associated plutons 229-216 Ma), and because of its strongly alkalic, shoshonitic geochemistry (Fig. 10). In general, Stuhini volcanic rocks are of high-K calc-alkaline to moderately shoshonitic character (Fig. 10b; Logan and Iverson, 2013). Very high, variable potassium contents are only seen in minor latite porphyries in the Dease Lake area (Logan and Iverson, 2013), in alkalic rocks from near the Dirk-Telena prospects in the lower Iskut area (Fig. 10b; Zagorevski et al., 2012), and in volcanic and intrusive rocks near the Galore Cu-Au porphyry deposit (Logan and Koyanagi, 1994). The sample suite from the upper volcanic unit of the Stuhini Group in the Scottie area ranges into these extremely potassic compositions.

The upper volcanic unit is approximately age-equivalent to: 1) the hanging wall breccia at the Granduc volcanogenic deposit (Mihalynuk et al., 2019); and 2) the alkalic volcanic/high-level

intrusive complex that hosts the Dirk and Telena showings in the lower Iskut River area (Fig. 1; Mihalynuk et al., 2011, 2012). Together, these rocks offer insights into possible tectonic and magmatic regimes in the Iskut region of Stikinia near the close of Stuhini volcanism. The Dirk-Telena alkalic igneous suite, the Zippa Mountain gabbro-syenite complex and the Newmont graben syenites are the southernmost expressions of the alkalic Galore trend (Fig. 1), which has been interpreted as a structurally controlled, post-subduction magmatic belt (Nelson and van Straaten, 2021). Granduc is adjacent to the north-striking, regional South-Unuk-Harrymel fault (Fig. 1), which forms the western margin of the Eskay rift (Middle Jurassic), and may mark the location of an earlier, syn-Stuhini back-arc or post-arc rift that hosted Granduc. The upper volcanic unit in the Scottie area, 18 km east of Granduc, shows that alkalic magmatism and formation of seabed massive sulphides in localized rift basins may have overlapped in time and space during the transitional period between Stuhini and Hazelton arc development. The modern Bismarck plate provides a possible analogy (Nelson et al., 2022, in press). Collision with the Australian plate in Papua New Guinea caused rotation of the Bismarck plate and development of complex back-arc rift (Manus basin) and fault geometries within it (Brandl et al., 2020). Seabed massive sulphides are currently forming in the Manus basin, while in another part of the back arc region (Tabar-Lihir-Tabar-Feni island chain), structurally controlled shoshonitic volcanism is accompanied by porphyry and epithermal mineralization (Brandl et al., 2020). The unusual and varied metal endowment of the Golden Triangle appears to be the product of an evolving arc-collisional environment that is only beginning to be understood. Observations of the Scottie gold mine area presented herein are a contribution to this ongoing work.

10. Conclusions

This study of the Scottie gold mine area has established a stratigraphic section of the Stuhini and Hazelton groups in the Stewart mining camp, 20 kilometres south of sections previously described on the flanks of the McTagg anticlinorium (Lewis, 2013; Nelson and Kyba, 2014). A mainly sedimentary unit in the Stuhini Group, similar to units seen in the McTagg area, is succeeded gradationally by ca. 214 Ma shoshonitic volcanic breccias, tuffs and flows. The base of the Hazelton Group is interpreted as unconformable and corresponds to a >10 m.y. depositional hiatus. The oldest Hazelton unit is a thin, local siliciclastic outlier that has a ca. 201 Ma maximum depositional age. Separately, a steeply east-dipping section of the Betty Creek Formation comprises two intervals of the Unuk River andesite unit and an intervening siltstone, the “upper siltstone unit” of Alldrick (1993). The upper siltstone unit has a ca. 191 Ma maximum depositional age and contains a Pliensbachian(?) ammonite mold. The stratigraphic section described here enables comparison of the early Mesozoic geological history of the Stewart mining camp with other regions of northwestern Stikinia and aids in tectonic reconstructions.

Acknowledgments

The management, board of directors, and employees of Scottie are thanked for their support over the past three years. This project would not have been possible without the collaboration of Thomas Mumford, Daniel Guestrin, and Jon Rigg of Scottie Resources Corp. LA-ICP-MS detrital zircon analysis was performed by Richard Friedman at the Pacific Centre for Isotopic and Geochronological Research (PCIGR) at the University of British Columbia. Careful reviews by Bram van Straaten and Rebecca Hunter have significantly improved this paper.

References cited

- Alldrick, D.J., 1993. Geology and metallogeny of the Stewart mining camp, northwestern British Columbia (104B, 103O). British Columbia Ministry of Energy, Mines and Petroleum Resources, British Columbia Geological Survey Bulletin 85, 105 p.
- Anderson, R.G., 1993. A Mesozoic stratigraphic and plutonic framework for northwestern Stikine (Iskut River area), northwestern British Columbia. In: Dunne, G.C. and McDougall, K.A., (Eds.), *Mesozoic paleogeography of the western United States, II*. Society of Economic Paleontologists and Mineralogists, Pacific Section, 71, pp. 477-494.
- Bird, S., Arseneau G., Petrovic, A., Palkovits, F., Fogarty, J., Jensen, S., Masson, B., Marsland, R., Teymouri, S., Grills, F., and Savage, K., 2020. Premier & Red Mountain gold project. Feasibility study NI 43-101 Technical Report. Prepared for Ascot Resources Ltd., 607 p. <<https://ascotgold.com/site/assets/files/4831/premier-and-red-mountain-gold-project-ni43-101-final-report-compressed.pdf>>
- Brandl, P.A., Hannington, M.D., Geerson, J., Peterson, S., and Gennerich, H.-H., 2020. The submarine tectono-magmatic framework of Cu-Au endowment in the Tabar-to-Feni island chain, PNG. *Ore Geology Reviews*, 121, 103491. <<https://doi.org/10.1016/j.oregeorev.2020.103491>>
- Brown, D.A., Gunning, M.H., and Greig, C.J., 1996. The Stikine project: Geology of western Telegraph Creek map area, northwestern British Columbia (NTS 104G/5, 6, 11W, 12 and 13). British Columbia Ministry of Energy, Mines and Petroleum Resources, British Columbia Geological Survey Bulletin 95, 176 p.
- Childe, F., 1997. Timing and tectonic setting of volcanogenic massive sulphide deposits in British Columbia: Constraints from U-Pb geochronology, radiogenic isotopes and geochemistry. Unpublished Ph.D. thesis, The University of British Columbia, 319 p.
- Cohen, K.M., Finney, S.C., Gibbard, P.L., and Fan, J.-X., 2013. The ICS International Chronostratigraphic Chart. *Episodes*, 36, 199-204 (updated version 2021/10, <<https://stratigraphy.org/ICSChart/ChronostratChart2021-10.pdf>>)
- Coulson, I.M., Russell, J.K., and Dipple, G.M., 1999. Origins of the Zippa Mountain pluton: A Late Triassic, arc-derived, ultrapotassic magma from the Canadian Cordillera. *Canadian Journal of Earth Sciences*, 36, 1415-1434. <<https://doi:10.1139/e99-045>>
- Coulson, I.M., Westphal, M., Anderson, R.G., and Kyser, T.K., 2007. Concomitant skarn and syenitic magma evolution at the margins of the Zippa Mountain pluton. *Mineralogy and Petrology*, 90, 199-221. <<https://doi:10.1007/s00710-006-0178-9>>
- Coutts, D.S., Mathews, W.A., and Hubbard, S.M., 2019. Assessment of widely used methods to derive depositional ages from detrital zircon populations. *Geoscience Frontiers* 10, 1241-1435. <<https://doi.org/10.1016/j.gsf.2018.11.002>>
- Cutts, J.A., McNicoll, V.J., Zagorevski, A., Anderson, R.G., and Martin, K., 2015. U-Pb geochronology of the Hazelton Group in the McTagg anticlinorium, Iskut River area, northwestern British Columbia. In: *Geological Fieldwork 2014*, British Columbia Ministry of Energy and Mines, British Columbia Geological Survey Paper 2015-1, pp. 87-102.
- Evenchick, C.A., 1991. Structural relationships of the Skeena Fold Belt west of the Bowser Basin, northwest British Columbia. *Canadian Journal of Earth Sciences*, 28, 973-983.
- Febbo, G.E., Kennedy, L.A., Savell, M., Creaser, R.A., and Friedman, R.M., 2015. Geology of the Mitchell Au-Cu-Ag-Mo porphyry deposit, northwestern British Columbia, Canada. In: *Geological Fieldwork 2014*, British Columbia Ministry of Energy and Mines, British Columbia Geological Survey Paper 2015-1, pp. 59-86.
- Febbo, G.E., Kennedy, L.A., Nelson, J.L., Savell, M.J., Campbell, M.E., Creaser, R.A., Friedman, R.M., van Straaten, B.I., and Stein, J.J., 2019. The evolution and structural modification of the superergian Mitchell Au-Cu porphyry, northwestern British Columbia. *Economic Geology*, 114, 303-324.
- Gagnon, J.F., Barresi, T., Waldron, J.W.F., Nelson, J.L., Poulton, T.P., and Cordey, F., 2012. Stratigraphy of the upper Hazelton Group and Jurassic evolution of the Stikine terrane, British Columbia. *Canadian Journal of Earth Sciences*, 49, 1027-1052.
- Greig, C., 2014. Latest Triassic-earliest Jurassic contractional deformation, uplift and erosion in Stikinia, NW BC. *Geological Society of America Abstracts with Programs*, 46, p. 588.
- Gunning, M.H., Hodder, R.W.H., and Nelson, J.L., 2006. Contrasting volcanic styles within the Paleozoic Stikine assemblage, western Stikine terrane, northwestern British Columbia. In: Colpron, M., and Nelson, J.L., (Eds.), *Paleozoic Evolution and Metallogeny of Pericratonic Terranes at the Ancient Pacific Margin of North America*, Canadian and Alaskan Cordillera. Geological Association of Canada, Special Paper 45, pp. 201-227.
- Henderson, J.R., Kirkham, R.V., Henderson, M.N., Payne, J.G., Wright, T.O., and Wright, R.L., 1992. Stratigraphy and structure of the Sulphurets area, British Columbia, In: *Current Research, Part A*, Geological Survey of Canada Paper 92-1A, pp. 323-332.
- Kyba, J., and Nelson, J., 2015. Stratigraphic and tectonic framework of the Khyber-Sericite-Pins mineralized trend, lower Iskut River, northwest British Columbia. In: *Geological Fieldwork 2014*, British Columbia Ministry of Energy and Mines, British Columbia Geological Survey Paper 2015-1, pp. 41-58.
- Irvine, T.N., and Baragar, W.R.A., 1971. A guide to the chemical classification of the common volcanic rocks. *Canadian Journal of Earth Sciences*, 8, 523-548.
- Le Bas, M.J., Le Maitre, R.W., Streckheisen, A., and Zanettin, B., 1986. A chemical classification of volcanic rocks based on the total alkali-silica diagram. *Journal of Petrology*, 27, 745-750.
- Le Maitre, R.W., Streckeisen, A., Zanettin, B., Le Bas, M.J., Bonin, B., Bateman, P., and Lameyre, J., 2002. *Igneous Rocks. A Classification and Glossary of Terms*, 2. Cambridge University Press, 236 p.
- Lepore, W.A., 2006. Temporal, isotopic, geochemical and structural studies of magmatism and associated mineralization within the Early to Middle Jurassic Hazelton Group on the Tide property, northwestern BC, Canada. Unpublished B.Sc. thesis, The University of British Columbia, 53 p.
- Lewis, P.D., MacDonald, A.J., and Bartsch, R.D., 2001. Hazelton Group/Bowser Lake Group stratigraphy in the Iskut River area: Progress and problems. In *Metallogenesis of the Iskut River area*, northwestern British Columbia, Mineral Research Unit Special Publication, Number 1, Chapter 2, pp. 9-30, The University of British Columbia.
- Lewis, P.D., 2013. Iskut River area geology, northwest British Columbia (104B/08, 09, 10 & part of 104B/01, 07, 11). *Geoscience BC Report 2013-05*.
- Logan, J.M., and Iverson, O., 2013. Dease Lake Geoscience Project: Geochemical characteristics of Tsaybahe, Stuhini and Hazelton volcanic rocks, northwestern British Columbia (NTS 104I, J).

- In: Geoscience BC Summary of Activities 2012, Geoscience BC Report 20-13-1, pp. 11-32.
- Logan, J.M., and Koyanagi, V.M., 1994. Geology and mineral deposits of the Galore Creek area (104G/3, 4). British Columbia Ministry of Energy, Mines and Petroleum Resources, British Columbia Geological Survey Bulletin 92, 95 p.
- Logan, J.M., Drobe, J.R., and McClelland, W.C., 2000. Geology of the Forrest Kerr-Mess Creek area, northwestern British Columbia, British Columbia Ministry of Energy and Mines, British Columbia Geological Survey Bulletin 104, 164 p.
- Ludwig, K., 2008. User's manual for Isoplot 3.70-a geochronological toolkit for Microsoft Excel. Berkeley Geochronology Center Special Publication 4, 76 p.
- MacDonald, A.J., 1993. Lithostratigraphy and geochronometry, Brucejack Lake, northwestern British Columbia (104B/08E). In: Geological Fieldwork 1992, British Columbia Ministry of Energy and Mines, British Columbia Geological Survey Paper 1993-1, pp. 315-323.
- MacDonald, S., 2021. Ore characterization of a mesothermal gold deposit in northwestern British Columbia. Unpublished B.Sc. Thesis, Kingston, Ontario, Queen's University, 63 p.
- McPhie, J., 1993. Volcanic textures: A guide to the interpretation of textures in volcanic rocks. Centre for Ore Deposit and Exploration Studies, University of Tasmania, 198 p.
- Mihalynuk, M.G., Logan, J.M., Zagorevski, A., and Joyce, N., 2011. Geology and mineralization of the Hoodoo Mountain area (NTS 104B/14E). In: Geological Fieldwork 2010, British Columbia Ministry of Energy and Mines, British Columbia Geological Survey, Paper 2011-01, pp. 37-64.
- Mihalynuk, M.G., Zagorevski, A., and Cordey, F., 2012. Geology of the Hoodoo Mountain area (NTS 104B/14W). In: Geological Fieldwork 2011, British Columbia Ministry of Energy, Mines and Natural Gas, British Columbia Geological Survey, Paper 2012-01, pp. 45-68.
- Mihalynuk, M.G., Zagorevski, A., Logan, J.M., Friedman, R.M., and Johnston, S.T., 2019. Age constraints for rocks hosting massive sulphide mineralization at Rock and Roll and Granduc deposits between Iskut and Stewart, British Columbia. In: Geological Fieldwork 2018, British Columbia Ministry of Energy, Mines and Petroleum Resources, British Columbia Geological Survey Paper 2019-01, pp. 97-111.
- Miller, E.A., Kennedy, L.A., and van Straaten, B.I., 2020. Geology of the Kinskuch Lake area and Big Bulk porphyry prospect, northwestern British Columbia: Syn-depositional faulting and basin formation during the Rhaetian (latest Triassic) transition from the Stuhini to the Hazelton Group. In: Geological Fieldwork 2019, British Columbia Ministry of Energy, Mines and Petroleum Resources, British Columbia Geological Survey Paper 2020-01, pp. 77-99.
- Morrison, G.W., 1980. Characteristics and tectonic setting of the shoshonite rock association. *Lithos*, 13, 97-108.
- Nadaraju, G., 1993. Triassic-Jurassic biochronology of the eastern Iskut River map area, northwestern British Columbia. Unpublished. M.Sc. thesis, The University of British Columbia, 258 p.
- Nadaraju, G., and Lewis, P.D., 2001. Biochronology data set, Chapter 8. In: Lewis, P.D., Toma, A., and Tosdal, R.M., (Eds.), Metallogensis of the Iskut River area, northwestern British Columbia. Mineral Deposit Research Unit, Special Publication Number 1, pp. 9-30.
- Nelson, J.L., and Kyba, J., 2014. Structural and stratigraphic control of porphyry and related mineralization in the Treaty Glacier-KSM-Brucejack-Stewart trend of northwestern Stikinia. In: Geological Fieldwork 2013, British Columbia Ministry of Energy, Mines and Natural Gas, British Columbia Geological Survey Paper 2014-1, pp. 111-140.
- Nelson, J.L., and van Straaten, B., 2021. Recurrent syn- to post-subduction mineralization along deep crustal corridors in the Iskut-Stewart-Kitsault region of western Stikinia, northwestern British Columbia. In: Sharman, E.R., Lang, J.R., and Chapman, J.B., (Eds.), Porphyry Deposits of the Northwestern Cordillera of North America: A 25-Year Update: Canadian Institute of Mining and Metallurgy Special Volume 57, pp. 194-211.
- Nelson, J.L., Colpron, M., and Israel, S., 2013. The Cordillera of British Columbia, Yukon and Alaska: Tectonics and metallogeny. In: Colpron, M., Bissig, T., Rusk, B.G., and Thompson, J.F., (Eds.), Tectonics, Metallogeny and Discovery: The North American Cordillera and Similar Accretionary Settings. Society of Economic Geologists Special Publication 17, Chapter 3, pp. 53-103.
- Nelson, J., Waldron, J., van Straaten, B., Zagorevski, A., and Rees, C., 2018. Revised stratigraphy of the Hazelton Group in the Iskut River region, northwestern British Columbia. In: Geological Fieldwork 2017, British Columbia Ministry of Energy, Mines and Petroleum Resources, British Columbia Geological Survey, Paper 2018-1, pp. 15-38.
- Nelson, J.L., Friedman, R., and van Straaten, B., 2021. LA-ICP-MS and TIMS U-Pb data files from the Iskut project (Dease Lake to Kitsault): British Columbia Ministry of Energy, Mines and Low Carbon Innovation, British Columbia Geological Survey GeoFile 2021-10, 13 p.
- Nelson, J.L., van Straaten, B., and Friedman, R., 2022. Latest Triassic-Early Jurassic Stikine-Yukon-Tanana terrane collision and the onset of accretion in the Canadian Cordillera: insights from Hazelton Group detrital zircon provenance and arc-back-arc configuration. *Geosphere*, in press.
- Pecerrillo, A., and Taylor, S.R., 1976. Geochemistry of Eocene calc-alkaline volcanic rocks from the Kastamonu area, northern Turkey. *Contributions to Mineralogy and Petrology*, 58, 63-81.
- Schaltegger, U., Guex, J., Bartolini, A., Schoene, B., and Ovtcharova, M., 2008. Precise U-Pb age constraints for end-Triassic mass extinction, its correlation to volcanism and Hettangian post-extinction recovery. *Earth Planetary Science Letters* 267, 266-275.
- Stanley, B., and Nelson, J.L., 2022. LA-ICP-MS U-Pb data files, detrital zircon geochronology, and geochemistry of the Stuhini and Hazelton groups, Scottie gold mine area, northwestern British Columbia. British Columbia Ministry of Energy, Mines and Low Carbon Innovation, British Columbia Geological Survey GeoFile.
- Tombe, S.P., Richards, J.P., Greig, C.J., Board, W.S., Creaser, R.A., Muehlenbachs, K.A., Larson, P.B., DuFrane, S.A., and Spell, T., 2018. Origin of the high-grade Early Jurassic Brucejack epithermal Au-Ag deposits, Sulphurets Mining Camp, northwestern British Columbia. *Ore Geology Reviews*, 95, 480-517.
- van Straaten, B.I., and Wearmouth, C., 2019. Geology of the Latham and Pallen Creek area, northwestern British Columbia: Distinguishing the Tsaybahe Group, Stuhini Group, and Hazelton Group, and the onset of Triassic arc volcanism in northern Stikinia. In: Geological Fieldwork 2018, British Columbia Ministry of Energy, Mines and Petroleum Resources, British Columbia Geological Survey Paper 2019-01, pp. 79-96.
- van Straaten, B.I., McLeish, D.F., and Harding, B.E., 2014. Diamond drilling, geological, geochemical, and geophysical work on the Tennyson property. British Columbia Ministry of Energy and Mines, Assessment Report 34816.
- Wotzlaw, J-F., Goex, J., Bartolini, A., Galley, Y., Krystyn, L., McRoberts, C.A., Taylor, D., Schoene, B., and Schalteffer, U., 2014. Towards accurate numerical calibration of the Late Triassic: High-precision U-Pb geochronology constraints on the duration of the Rhaetian. *Geology* 42, 571-574.
- Zagorevski, A., Mihalynuk, M.G., and Logan, J.M., 2012. Geochemical characteristics of Mississippian to Pliensbachian volcanic and hypabyssal rocks in the Hoodoo Mountain area (NTS

104B/14E). In: Geological Fieldwork 2011, British Columbia
Ministry of Energy, Mines and Natural Gas, British Columbia
Geological Survey, Paper 2012-01, pp. 121-133.